

CrossMark  
click for updatesCite this: *Catal. Sci. Technol.*, 2016,  
6, 3670

## Nitrogen-doped porous carbon materials: promising catalysts or catalyst supports for heterogeneous hydrogenation and oxidation

Mingming Li, Fan Xu, Haoran Li and Yong Wang\*

Developing novel and efficient catalysts is a critical step in common heterogeneous hydrogenation and oxidation reactions. Despite the frequent study of metal oxide-supported catalysts, porous carbon materials have also emerged as valuable potential catalysts. However, due to their highly microporous structures and inferior structural functionalities, traditional activated carbons (ACs) have become increasingly less popular for industrial applications. To deal with the disadvantages of ACs, tremendous efforts have been made to develop novel nitrogen-doped porous carbon (NPC) materials with novel features such as highly porous structures and abundant structural nitrogen heteroatom decoration. As catalysts or catalyst supports, NPC materials have shown superior activities in many applications covering a wide range of heterogeneous hydrogenation and oxidation reactions. In this contribution, we review the fabrication methods for NPC materials used in heterogeneous hydrogenations and oxidations and highlight the intrinsic catalytic mechanisms along with the catalyst design strategies.

Received 11th March 2016,  
Accepted 31st March 2016

DOI: 10.1039/c6cy00544f

[www.rsc.org/catalysis](http://www.rsc.org/catalysis)

### 1. Introduction

As early as 1836, Berzelius introduced the term “catalysis.” Catalysts possess special powers to influence the affinity of chemical substances. Since then, catalysts have been involved in a large number of societal developments. Among various catalysts, heterogeneous catalysts that are not soluble in the reaction mixture possess the inherent advantage of easy separation and better handling properties, thus showing promising industrial value. It is no exaggeration to say that heterogeneous catalysts have been involved in almost all large-scale productions of inorganic and organic chemicals, crude oil refinement, environmental protection, and energy conversion.<sup>1,2</sup> From this point of view, beyond the simple chemical transformation of chemicals, we can envision that heterogeneous catalysts may hold the key to the creation of a cleaner and more sustainable world.

The frequently employed reaction types in the industrial manufacturing of chemicals cover many selective hydrogenation and oxidation reactions, which are particularly necessary in the activation of a wide range of raw materials to produce useful products or intermediates.<sup>1</sup> Hydrogenation is a common process to reduce organic compounds such as phenol,<sup>3,4</sup> and oxidation is another important process to functionalize substrates (*e.g.*, the industrial oxidation of propene to acrolein).<sup>5</sup>

However, some traditional hydrogenations employing simple metal oxide catalysts usually require high temperatures and high H<sub>2</sub> pressures, and oxidation reactions use stoichiometric oxidants such as dichromate, permanganate and toxic oxides, which are rather harmful to the environment.<sup>6–8</sup> Therefore, with the increased focus on environmental protection and energy conservation, the pursuit of greener chemical transformation strategies *via* the invention of active and powerful heterogeneous catalysts has become a focus of scientific research.

Indeed, scientists have already devoted considerable effort to the reformation of catalysts used in traditional industrial hydrogenation and oxidation processes. For example, commercial cyclohexanone production typically involves either the oxidation of cyclohexane<sup>3,9,10</sup> or the hydrogenation of phenol in a “one-step” or “two-step” process,<sup>11,12</sup> generating undesirable byproducts that lower the product yield and complicate the recovery/separation steps. Therefore, the one-step and selective direct hydrogenation of phenol to cyclohexanone is preferable; a recent work accomplished this task by employing a g-C<sub>3</sub>N<sub>4</sub>-supported Pd catalyst under atmospheric pressure of hydrogen at room temperature.<sup>13</sup> As for oxidation, the change in the stoichiometric use of MnO<sub>2</sub> for the production of citral (a key intermediate for fragrances and vitamins A and E) using Ag-supported catalysts, which is more atom-efficient and environmentally friendly, was pursued by BASF.<sup>14</sup> These were the very limited endeavors in reforming catalysts in industrial hydrogenation and oxidation reactions. With respect to the catalysts in hydrogenation reactions, different metals such as noble metals Pd, Au, Ru, Pt and Ir and

Advanced Materials and Catalysis Group, ZJU-NHU United R&D Center,  
Department of Chemistry, Zhejiang University, Hangzhou 310028, PR China.  
E-mail: [chemistry@zju.edu.cn](mailto:chemistry@zju.edu.cn)

non-noble metals Fe, Ni, Co and Cu showed diverse catalytic performances. The catalyst supports, including metal oxides,<sup>15</sup> zeolites,<sup>16</sup> metal-organic frameworks (MOFs)<sup>17</sup> and carbons in different forms, have also witnessed great development.<sup>18</sup> As for oxidations, the heterogeneous catalysts included many metal-free catalysts such as metal oxides,<sup>19</sup> carbon nitride materials<sup>20</sup> and carbons (*e.g.*, CNTs and activated carbons),<sup>18</sup> and noble metal (*e.g.*, Pd or Au)-supported catalysts are currently booming.<sup>21–23</sup> Since the early practice of employing a nitrogen containing g-C<sub>3</sub>N<sub>4</sub> support depositing Pd nanoparticles (NPs) in heterogeneous hydrogenation, which demonstrated the importance of the interaction of nitrogen heteroatom with Pd in promoting catalytic activity,<sup>13</sup> nitrogen-doped porous carbon (NPC) materials have drawn intensive attention in heterogeneous hydrogenations and oxidations as catalysts or catalyst supports.<sup>24–33</sup> Conventional porous carbon materials such as activated carbon (AC) was traditionally synthesized through pyrolysis and the physical or chemical activation of raw materials such as coal, wood or fruit shells at elevated temperatures.<sup>34,35</sup> AC has long been used as an excellent sorbent and support for NPs in catalytic reactions<sup>36,37</sup> due to its various valuable properties: high specific area, large pore volume, different available surface properties such as heteroatom doping and hydrophilicity, and low cost. Thanks to a better understanding of the physico-chemical properties of carbon as a catalyst support, the industrial use of AC as a catalyst support has been extended to new areas such as environmental protection (*e.g.*, volatile organic compound oxidation<sup>38</sup>), selective oxidation<sup>39</sup> and hydrogenations.<sup>40</sup> Despite its wide range of newly developed applications, AC still suffers from limitations arising from the methods used in the production. The main drawbacks are as follows: 1) the pores are restricted mainly to micropores with a very narrow size distribution, which limits the mass transfer of molecules in reactions; 2) the micropores (<2 nm) largely restrict the full utilization of deposited NPs (usually >2 nm), causing the NPs to disperse only on the carbon surface and further aggregate and leach easily; 3) the architecture and nano-dimensions of AC cannot be easily tuned for specific catalytic uses; and 4) the surface functional groups need to be further tailored for specific needs by secondary functionalization to create, for example, N-containing groups.

To overcome the abovementioned limitations, nitrogen-doped porous carbon materials have recently become a subject of particular interest to researchers. Because they have witnessed enhanced performance in various applications, such as serving as electrodes in metal-free oxygen reduction reaction,<sup>41</sup> supercapacitor test,<sup>42</sup> and acting as metal-free catalysts or catalyst supports in catalytic reactions.<sup>32,43</sup> Generally, there are two ways to synthesize NPC: 1) the heat treatment of undoped porous carbon materials under nitrogen-containing atmosphere; and 2) the direct synthesis from nitrogen-containing precursors or a mixture of carbon- and nitrogen-containing precursors. Various fabrication techniques has been reported: a) replication synthesis with pre-synthesized hard templates such as mesoporous silica or

other ordered and disordered metal oxides through impregnation, carbonization and template removal;<sup>44,45</sup> b) metal salt-assisted fabrication through the carbonization of a mixture of carbon precursors and metal salt followed by water washing;<sup>46–48</sup> c) self-assembly using soft templates such as P123 or F127 through condensation and carbonization;<sup>49–51</sup> and d) direct synthesis such as Starbon materials synthesis using a freeze-drying technique.<sup>52</sup> Generally, nitrogen functionalities provide basic properties, which can enhance the interaction between carbon surfaces and reaction molecules.<sup>40,53</sup> Further, nitrogen doping was able to enhance the hydrophilicity of NPC, which may greatly improve catalyst dispersion in aqueous media and in turn contribute to a better catalytic performance.<sup>43</sup> Moreover, the spin density and charge distribution of carbon atoms will be influenced by the neighboring nitrogen dopants,<sup>32,54</sup> which may create increased defects and more active sites. On one hand, these newly created defects (such as N-containing functional groups) have enabled NPC materials to be desired catalysts in the metal-free oxidation reactions.<sup>32,33,55,56</sup> On the other hand, the electronegativity introduced in the carbon structure because of the doped nitrogen may stabilize deposited metal with small size and narrow distribution and increase the metal-carbon binding energy. This in turn enhances the catalytic activity and reaction stability of the resulting NPC-supported catalyst in heterogeneous catalytic reactions, especially in the oft-investigated heterogeneous hydrogenations and oxidations.<sup>24,31,43</sup> Therefore, in addition to N-CNTs<sup>57</sup> and N-graphene<sup>58</sup> in the NPC family, new generations of NPC materials are also promising catalysts or catalyst supports because of their excellent properties, ease of handling and large-scale production.

To date, nitrogen-doped carbon materials have already been reviewed in some exciting papers,<sup>59–62</sup> and reviews on the synthesis, properties and applications of N-graphenes and N-CNTs have been frequently reported.<sup>58,63,64</sup> However, their emphases were largely placed on the applications for energy conversion and storage, with less space for catalytic reactions, particularly catalytic hydrogenations and oxidations. Notably, an excellent systematic review on the catalytic uses of nanocarbon was recently provided by Su *et al.*, who forecast a bright future in catalysis using nanocarbon-based materials.<sup>18</sup> The introduction of nitrogen-doped porous carbon materials as catalysts or catalyst supports in heterogeneous hydrogenation and oxidation reactions has been a research hot spot in recent years. However, until now, the significant progress made in this area has not been specifically reviewed. Therefore, it is urgent to write a review to systematically introduce the various fabrication methods of nitrogen-doped porous carbon materials and their endless applications in heterogeneous hydrogenations and oxidations. Thus, we would like to provide a review regarding the catalytic oxidations and hydrogenations based on NPC materials and highlight the catalytic mechanisms along with catalyst design strategies (*e.g.*, developing NPC-based composite-supported catalysts<sup>65</sup> or bimetallic catalysts<sup>66</sup>) with the hope

that more breakthroughs will be achieved in this direction and boost the used of heterogeneous catalysis in sustainable chemistry.

## 2. Fabrication of nitrogen-doped porous carbons

The intrinsic drawbacks of activated carbons described above largely restrict their industrial use. In the field of catalysis, most activated carbons are used for the synthesis of Pd/AC catalysts toward hydrogenation processes.<sup>18</sup> This inspired chemists to construct carbon materials with controlled porosities and chemical functionalizations (*e.g.*, decoration with nitrogen heteroatoms), resulting in advanced catalytic activity together with improved product selectivity.<sup>31,32,43,55,67</sup> In this section, we discuss the various fabrication techniques for generating NPC materials tested in catalytic reactions. More specifically, emphasis will be placed on heterogeneous catalysis (mainly hydrogenations and oxidations) related to the synthesis of nitrogen-doped porous carbon as there have been many excellent reviews on the synthesis of porous carbons<sup>68–74</sup> and nitrogen-doped carbons showing endless prospects in electrochemical applications.<sup>59,60</sup> To incorporate nitrogen into NPC materials, two fabrication methods are generally used: post treatment and direct synthesis. Particularly, post treatment is done through reactions with nitrogen-containing reagents (*e.g.*,  $\text{NH}_3$  and amines), while direct synthesis is typically completed by the direct carbonization of nitrogen-rich carbon precursors or carbon precursors mixed with nitrogen dopants. Fig. 1 shows the various nitrogen functionalities that will be mentioned in this review.

### 2.1 Post-treatment synthesis

Constricted by the innately inferior characteristics of undecorated carbon, it is highly desirable to functionalize

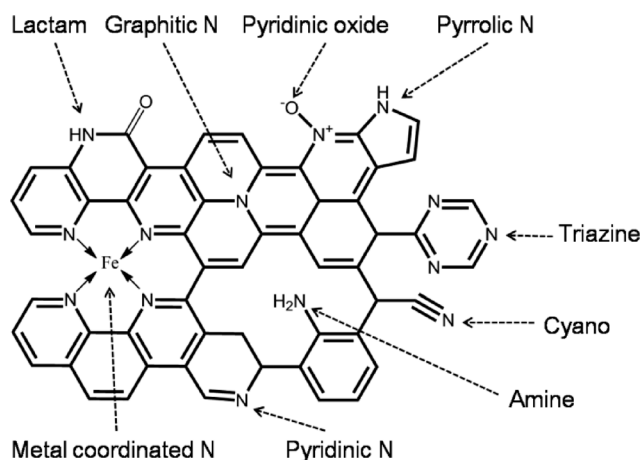


Fig. 1 The various types of nitrogen functionalities observed in the NPC materials discussed in this review. The most frequently noted types are pyridinic, pyrrolic and graphitic nitrogen groups. Others include amine, cyano, lactam, triazine, pyridinic oxide and metal-coordinated nitrogen groups.

carbons in successive steps *via* reactions with nitrogen-containing reagents to improve the catalytic performance. Among the various reagents employed,  $\text{NH}_3$  is by far the most frequently used to introduce nitrogen into porous carbons.<sup>33,55,56,75–78</sup> Considering the possibly similar functions of  $\text{NH}_3$ , a series of amines including urea, melamine, dicyandiamine, DMF, ethylenediamine,  $\text{N}_2\text{H}_4$ ,  $\text{NH}_3\cdot\text{H}_2\text{O}$  and nitrates have also been used.<sup>24,40,79–93</sup> Some other reagents such as acetonitrile<sup>32</sup> and different kinds of nitrogen-containing organic ligands<sup>94,95</sup> have also been studied. Depending on the reagents and the treatment conditions, the final physicochemical properties, pore structures and the content and types of nitrogen functionalities may vary, possibly resulting in significant changes in the electronic state of the carbon surface and the deposited metal NPs and, finally, the catalytic performance.

During high-temperature treatments, ammonia decomposes to free radicals such as  $\text{NH}_2$ ,  $\text{NH}$ , and atomic nitrogen and hydrogen.<sup>96</sup> These radicals can etch carbon fragments leading to increased porosity. They can also replace oxygen-containing species on the carbon to form surface groups such as pyridinic, pyrrolic and quaternary nitrogen functionalities. The promoting effect of nitrogen doping in the carbons originally encouraged researchers to increase the doping content; the gaseous-phase treatment of carbons in  $\text{NH}_3$  atmosphere with controlled reaction time and temperature offers a good option to do so. In this way, the nitrogen content can easily reach up to  $\sim 9$  wt%,<sup>24</sup> although most work reported low values below 5 wt%.<sup>33,55,75,78,83,97</sup> In some cases, a higher content of nitrogen results in a higher activity.<sup>33</sup> The introduction of nitrogen heteroatoms is indeed helpful; however, it is not always beneficial to have a high nitrogen content, and a specific nitrogen functionality may play a critical role.<sup>55,56,76,97</sup> Wang and coworkers prepared three different nitrogen-doped graphene nanosheets (NG) *via* the treatment of GO in  $\text{NH}_3$  under different temperatures (800–1000 °C) and tested them for the metal-free aerobic selective oxidation of benzyl alcohols.<sup>97</sup> The nitrogen content decreased with increasing temperature. However, NG-900 demonstrated the highest activity, and the active centers were found to be graphitic  $\text{sp}^2$  nitrogen sites. Notably, in many reported works, pyridinic and pyrrolic nitrogen species are dominant under  $\text{NH}_3$  treatment, whereas minor species such as graphitic nitrogen may be more active in reactions.<sup>55,76,97</sup>

In addition to  $\text{NH}_3$ , other kinds of amines are also widely used. Among the various amines used, urea and melamine seems to be the most frequently studied,<sup>24,40,53,80,82,83</sup> partly due to their low cost and ability to offer a relatively high nitrogen doping level up to  $\sim 20$  wt%. For example, Li's group reported that the nitrogen content can reach 18.56 wt% by treating AC with melamine at 600 °C (NAC-600), while only 7 wt% nitrogen was observed in NAC-800 (AC treated with melamine at 800 °C).<sup>40</sup> Similar to the gaseous phase functionalization of carbons in  $\text{NH}_3$ , Ma's group efficiently doped nitrogen into a layered carbon framework through a CVD process (1073 K) using an  $\text{N}_2$  stream saturated with

acetonitrile vapor as the nitrogen source.<sup>32</sup> The content of nitrogen in the product could be adjusted by varying the exposure time to the acetonitrile/N<sub>2</sub> stream (from 30 min to 900 min), and the nitrogen content easily reached up to 8.9 wt%. When applying the resulting nitrogen-doped catalysts (referred to as LCN) in the metal-free selective oxidation of ethylbenzene, remarkably improved catalytic activity as well as a greatly increased acetophenone selectivity were observed, and the activity and yield of the targeted product appeared to be more in line with the nitrogen content. In fact, the positive relationship with total nitrogen content was coincident because detailed investigations demonstrated that the incorporated graphitic-type nitrogen is pivotal for the C–H bond activation reaction, in which the incorporated nitrogen atoms are preferentially bound at graphitic sites in the carbon framework under high-temperature annealing. The present work may offer valuable guidance for the accurate control of the graphitic-type nitrogen content of NPC materials for targeted uses because the graphitic nitrogen content is correlated with the amount of total nitrogen.

Inspired by the idea of preparing novel heterogeneous nanostructured catalysts from defined homogeneous organometallic complexes, the Beller group creatively converted homogeneous cobalt complexes into heterogeneous cobalt oxide catalysts *via* immobilization and pyrolysis on activated carbon, creating a Co<sub>3</sub>O<sub>4</sub>–N/C catalyst that demonstrated superior catalytic activity in the nitroarene hydrogenation.<sup>95</sup> Various organic nitrogen ligands were initially selected to finely coordinate with the Co and control the Co particle size, but they also happened to act as nitrogen sources for obtaining nitrogen-doped carbons. The structures of the nitrogen ligands played great roles in the resulting Co<sub>3</sub>O<sub>4</sub>–N/C catalysts. The most active catalyst in the hydrogenation of nitroarenes was observed by employing 1,10-phenanthroline as the nitrogen ligand, and a wide range of substituted nitroarenes were tested. Later, the same group changed cobalt salt to iron salt for the preparation of a nanoscale iron oxide supported on a nitrogen-doped carbon catalyst for the investigation of nitroarene hydrogenation.<sup>27</sup> This time, the authors found that the coordinated nitrogen centers (FeN<sub>x</sub>) governed the catalytic activity, while the sizes of the iron oxide particles seemed to play a minor role. With the striking discovery of a new active center (metal coordinated nitrogen) in heterogeneous catalysts based on Co (Fe) coordinated with nitrogen-doped carbon, this catalysis system was further applied for a wide range of catalytic reactions covering diverse compounds such as selective hydrogenation, oxidation and oxidative dehydrogenation reactions.<sup>28,29,94,98–103</sup>

## 2.2 Direct synthesis

Compared with post-treatment methods, which require more than two synthetic steps, direct synthesis offers a more convenient, one-step way to prepare targeted NPC materials. Typically, direct synthesis is completed in two ways: 1) direct carbonization of nitrogen-rich carbon precursors, where the

precursors are typically molecules containing cross-linkable groups such as –CN and –NH<sub>2</sub>,<sup>32,104,105</sup> nitrogen-rich polymers,<sup>106–109</sup> ionic liquids,<sup>43,110</sup> and biomass derivatives;<sup>26,43,111</sup> 2) direct carbonization of carbon precursors mixed with nitrogen dopants, where added nitrogen co-reagents including a series of amines such as NH<sub>3</sub>, melamine, urea and aniline are also used in the post-treatment method.<sup>30,104,112–124</sup> Both of these strategies facilitate the incorporation of nitrogen functionalities throughout the entire carbon structures in a more homogeneous way and thus contribute to more stable nitrogen functionalities compared with surface doping *via* post-synthetic methods. In summary, they offer more stable and homogeneous properties that are critical for catalytic reactions. Hence, tremendous efforts have been devoted to the selection of desired precursors (or co-reagents) assisted by a series of fabrication techniques (*e.g.*, hard-template, soft-template, and template-free techniques) for the one-step fabrication of NPC materials that are active in catalytic reactions. Therefore, we would like to discuss the direct fabrication of NPC materials based on the above fabrication techniques.

**2.2.1 Hard-template methods.** The synthesis of mesoporous carbon materials was first reported by Knox and co-workers in the early 1980s using a spherical solid gel as the hard template.<sup>44</sup> Their approach, which is often used today for the hard-template synthesis of mesoporous carbons, includes the following steps: a) preparation of silica gel with controlled pore structure; b) impregnation/infiltration of the silica template with monomer or polymer precursors; c) cross linking and carbonization of organic precursors; and d) dissolution of the silica template. This method has the advantages of finely controlling the pore structure of the final carbon materials by simply adjusting the morphology of the silica template and has proven beneficial for the catalytic performance due to improved mass transfer. Later, the groups of Ryoo and coworkers introduced ordered mesoporous carbons by employing ordered aluminum silica MCM-48 templates,<sup>45</sup> further advancing the area of porous carbon for catalytic applications due to the faster mass transfer in large and uniform pores. These controlled synthetic methods thus attracted intensive attention for the synthesis of nitrogen-doped porous carbon with designed pore structures, demonstrating excellent performance in various fields, particularly in heterogeneous catalytic hydrogenations and oxidations.

The advantages of silica templates brought intensive investigations of fabricating NPC materials for heterogeneous catalysis. An early work by Dai *et al.* employed spherical silica as the hard template and the biomolecule dopamine as the precursor to successfully generate spherical and uniform hollow carbons with apparent nanocapsules.<sup>111</sup> Inspired by the large cavities of these hollow carbons, this strategy was applied to fabricate a carbon-coated Au catalyst (Fig. 2), which was used as a nanoreactor in the catalytic reduction of 4-nitrophenol. Although this work did not mention the function of nitrogen doping in the carbon skeleton, nitrogen heteroatoms were indeed incorporated into the carbon

skeletons.<sup>125</sup> However, the use of large silica spheres as hard templates for the preparation of hollow NPC-based heterogeneous catalysts was scarcely seen thereafter,<sup>125,126</sup> partly due to the difficulty in controlling the thickness of the carbon shell. More importantly, the limited mesoporous channels into the hollow cavity largely restricted the full use of the surface, leading to inferior mass transfer and weak reactivity.

Considering that the hollow closed cavities of the produced NPC materials using large silica spheres as the templates are hardly accessible, the preparation of NPC with sufficient and more accessible mesopores through silica templating has received more attention, covering nitrogen-rich carbon precursors<sup>26,43,110,127–130</sup> and coreagents.<sup>119</sup> For example, Wang's group employed nitrogen-rich ionic liquids (ILs) as the precursors and small colloidal silica nanospheres (Ludox HS-40) as the sacrificial template to successfully generate NPC materials with nitrogen contents of up to 15 wt%. These NPC materials functioned as a desirable support for Pd NPs, demonstrating superior catalytic activity in phenol and vanillin hydrogenations.<sup>43,110</sup> These studies mainly resulted in interconnected but disordered mesopores; thus, scientists further devoted energies to designing ordered pores, which are supposed to be more advantageous in catalysis. The group of Ma used a self-assembly method by mixing a nitrogen-containing IL (C16MIMBr) with TEOS in NaOH solution followed by filtration, carbonization and acid etching; an MCM-41-like ordered 2D hexagonal NPC material with bimodal mesopores (about 3.8 and 9.0 nm) was obtained.<sup>129</sup> This one-step assembly strategy was more facile than their later developed SBA-15 templated method for fabricating or-

dered nitrogen-doped dual mesoporous carbon,<sup>130</sup> which was frequently used to synthesize ordered carbon materials.<sup>131</sup> Restricted by the high cost of ILs, biomass-derived nitrogen-containing precursors, which are renewable and naturally available, have recently caught the eyes of researchers. For example, the hydrothermal treatment of chitosan-derived glucosamine hydrochloride followed by high-temperature carbonization produced an NPC with a moderate nitrogen content of ~7 wt%; this NPC served as a support for Pd or alloy RuPd NPs, which demonstrated excellent performance in the selective hydrogenation of benzoic acid and derivatives.<sup>26,128</sup> However, toxic H<sub>2</sub>F or NH<sub>4</sub>HF or NaOH is often used to dissolve the silica in hard-template methods based on silica, which poses additional threats to the environment. The group of Schüth synthesized highly porous nitrogen-doped carbons *via* the direct hydrothermal carbonization and thermal treatment of lobster exoskeleton followed by etching the CaCO<sub>3</sub> template in acetic acid solution. This method was milder and more sustainable.<sup>132</sup>

**2.2.2 Metal salt-assisted methods.** The recently developed molten salt-assisted fabrication methods, which can also be called “salt templating syntheses”, have been used to produce porous carbons.<sup>46,47,133–135</sup> Typically, a non-carbonizable inorganic salt is mixed with a carbon precursor (such as glucose or ionic liquids), which is condensed and scaffolded in the presence of the molten salt at elevated temperatures. The salt phase is easily removed by simple washing with water, which results in highly porous carbons with the desired structural and chemical functionalities.<sup>46,47</sup> In contrast to the hard-templating method, the employed salt template can be readily recycled for another run. This method allows for the easy fabrication of functionalized porous carbons, which may show promise in heterogeneous catalytic hydrogenations. Therefore, by choosing the proper nitrogen source, NPC materials can be obtained. For example, NPC materials with nitrogen contents of up to 11.9 wt% and high specific areas of up to 1800 m<sup>2</sup> g<sup>-1</sup> can be readily obtained by simply adding melamine as the nitrogen-containing source.<sup>134</sup> These NPC materials were used as efficient metal-free catalysts in the oxidation of a wide range of aryl alkanes in the aqueous phase with *tert*-butyl hydroperoxide (TBHP) as the oxidant.

Inspired by the fact that bread making involves the use of a gas-producing reagent to produce porosity in the bread, Wang's group used a gas-producing metal salt (KHCO<sub>3</sub>) to obtain highly porous carbon structures after carbonization with carbon precursors.<sup>48</sup> Typically, the employed KHCO<sub>3</sub> expands and etches the carbon framework during high-temperature carbonization, known as a “leavening” strategy. Well-developed 3D hierarchically porous carbons (with *S*<sub>BET</sub> up to 1893 m<sup>2</sup> g<sup>-1</sup>) consisting of macro-, meso- and micropores from a wide range of biomass derivatives (xylose, glucose, sucrose, cellulose, starch, and chitin) and even crude biomass (such as straw and bamboo) were produced (Scheme 1). We believed that this method could be applied to the synthesis of 3D hierarchical NPC materials from inexpensive nitrogen-

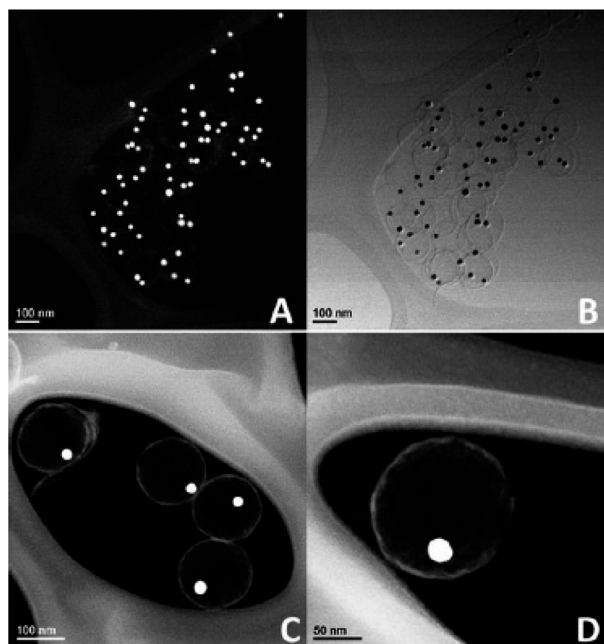


Fig. 2 STEM images of Au@C yolk-shell nanocomposites: A), C) and D) Z-contrast and B) bright-field images. Reproduced with permission from ref. 111. Copyright© 2011 WILEY-VCH Verlag GmbH & Co. KGaA, Weinheim.

containing crude biomass, where the NPC serving as a promising catalyst support can be expected.

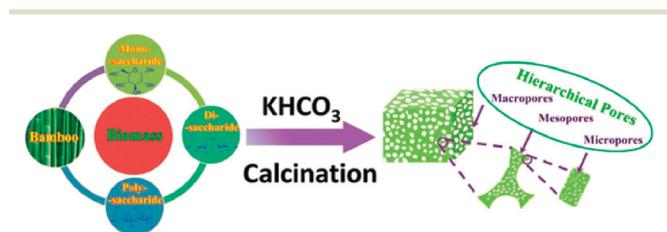
**2.2.3 Soft-template methods.** As an alternative to the hard-templating method, the soft-templating method successfully avoids the toxic and corrosive chemicals frequently used in hard-templating methods. Thus, the so-called soft template, usually micelles of amphiphilic block-copolymers such as PS-*b*-P4VP, F127 and P123, is more likely to be readily decomposed to generate *in situ* pores during high-temperature carbonization.<sup>49–51</sup> As phenol and formaldehyde were frequently selected as precursors for amphiphilic block copolymer-based porous carbons,<sup>49–51</sup> a few works were also reported on the fabrication of F127- and phenol-based NPC materials and their use in catalytic reactions.<sup>115,136</sup> The fast development of material science has thus further extend the scope of soft templates beyond those traditional block-copolymers, covering alternatives such as melamine or urea,<sup>114,120</sup> poly(vinyl pyrrolidone)<sup>108</sup> and poly(ionic liquid)s.<sup>25,31,137</sup> It is also noteworthy that the traditional phenol- and formaldehyde-based soft-templated NPC materials are highly recommended to be replaced by more sustainable carbon precursors with improved fabrication techniques.<sup>25,30</sup>

Lu and coworkers added 1,6-diaminohexane as a nitrogen source into a solution of resorcinol, F127 and formaldehyde; this compound could also help to better adsorb and stabilize Pd. A Pd@NPC catalyst was successfully obtained and demonstrated mild benzyl alcohol oxidation performance.<sup>115</sup> A modified phenol- and formaldehyde-based method was developed. Ordered NPC was prepared through an aqueous self-assembly process with F127 as a soft template, 1,3,5-trimethylbenzene as the morphological control agent, and 3-aminophenol as a carbon and nitrogen source. The material exhibited excellent catalytic performance for the selective oxidation of ethylbenzene.<sup>136</sup> The Figueiredo group employed resorcinol and formaldehyde (RF) as carbon precursors and melamine or urea as the soft template. Through gelation and high-temperature (500–900 °C) carbonization, a series of NPC xerogels were obtained that showed improved catalytic abilities in advanced oxidation processes.<sup>114,120</sup> The melamine or urea here may function both as a soft template and as a nitrogen source. However, the pores were largely restricted to micropores due to the easy collapse of the cross-linked framework resulting from the weak interaction of melamine (urea) with RF. Discarding the use of phenol and formalde-

hyde to fabricate NPC materials, a recent electron spinning method employed polyacrylonitrile (PAN) as carbon, nitrogen source and poly(vinyl pyrrolidone) (PVP) as soft template was developed. Through high-temperature carbonization, they successfully created porous nitrogen-doped carbon fibers (N@CFs).<sup>108</sup> Here, PVP functions as a sacrificial template that is responsible for the porosity; the pores are mostly constituted by a network of meso- and macropores. Although a low specific area (20 m<sup>2</sup> g<sup>-1</sup>) was observed, the material still showed good activity towards the oxidation of H<sub>2</sub>S to S.

The increased focus on sustainable chemistry generates the need for alternative synthetic methodologies such as precursor modification. Thus, carbohydrate-based carbon materials have attracted intensive attention.<sup>69,71,138</sup> Nonetheless, the serious aggregation and weak assembly ability of carbohydrate-derived carbon materials commonly lead to the formation of irregular bulk carbon spheres, which are nonporous and have an unfavorably low surface area (<20 m<sup>2</sup> g<sup>-1</sup>).<sup>139–141</sup> Thus, efficient methods are required to induce abundant pores in the final carbons, particularly NPC materials. As an interesting contribution towards this end, the Wang group initially employed poly(ionic liquid)s (PILs) as additives to improve the hydrothermal carbonization (HTC) of carbohydrates (such as glucose and fructose) and prepare NPC materials.<sup>25,31</sup> These PILs played many different roles in this process, that is, as stabilizer, pore-generating agent, and nitrogen source. Thus, the aggregation of carbohydrate-derived carbon domains in the carbonization was effectively avoided, and NPC materials with an improved *S*<sub>BET</sub> of up to 572 m<sup>2</sup> g<sup>-1</sup> and a high nitrogen content of up to 4.8 wt% were obtained.<sup>25</sup> However, it is notable that the HTC products always require further high-temperature carbonization for wider applications, thus complicating the fabrication process. Therefore, soft template-based one-step fabrication methods for the preparation of biomass-derived NPC materials are highly preferable. Using melamine as a soft template, non-noble metal (Co or Ni)-containing NPC materials were fabricated via the carbonization a mixture of biomass-derived glucosamine hydrochloride, non-noble metal salts and melamine in a one-step carbonization process. The produced NPC materials were directly employed as desired catalysts in the hydrogenation and dehydrogenation reactions.<sup>30,142,143</sup>

**2.2.4 Template-free methods.** The direct transformation of carbon precursors to porous NPC materials was developed as an attractive alternative to traditional hard- or soft-template methods. The difficulty lies in maintaining the preformed pore structures of the precursors or the *in situ* formed porous framework upon carbonization. However, it is not easy to obtain highly porous NPC materials that are more advantageous for catalytic applications. For example, nonporous nitrogen-doped carbon nanospheres were prepared *via* the direct thermal pyrolysis of aniline or nitrobenzene under 1223 K for 2 h. After the deposition of nickel NPs, the obtained catalysts were tested in the gas phase hydrogenation of butyronitrile.<sup>144</sup> Apparent nickel sintering was observed, partly because the non-porosity cannot effectively confine the



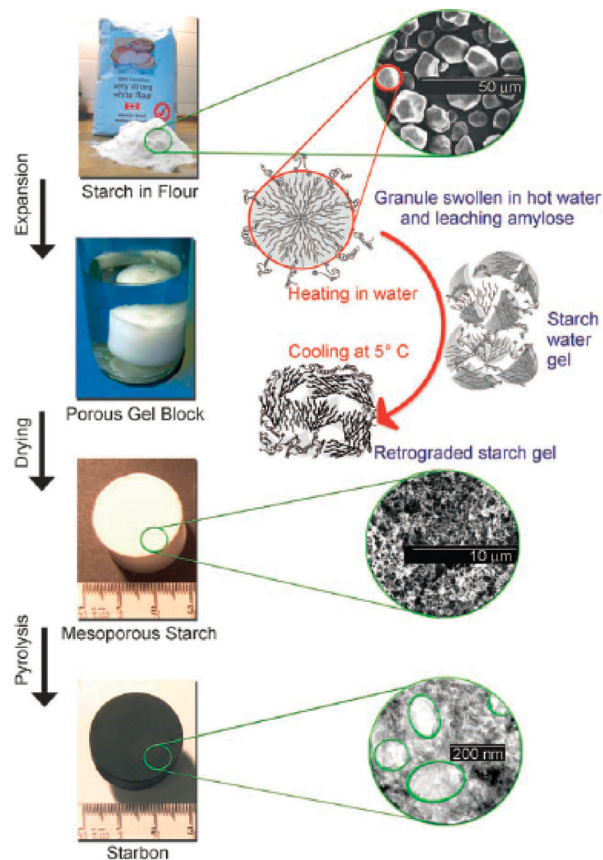
**Scheme 1** Schematic diagram of the formation of Cx-LE: mixing the biomass with the “leavening” agents followed by calcination under an inert gas for the synthesis of Cx-LE. Reproduced with permission from ref. 48. Copyright© 2015 The Royal Society of Chemistry.

NPs despite the effect of the doped nitrogen. Using a hydrothermal carbonization method combined with a following freeze-drying process, nitrogen-containing carbon precursor poly(2-aminothiazole) was successfully transformed into a N, S-codoped meso- and macroporous carbon. However, it is more preferable to call it a carbonaceous polymer because of the low carbonization temperature (180 °C), where it is suspicious for porosity maintenance when sent to high-temperature carbonization.<sup>109</sup> Therefore, the careful selection of carbon precursors and preferable condensation methods are required for the direct synthesis NPC materials.

Recently, Li's group used porous cobalt containing MOFs (ZIF-67) as the sacrificial precursor and successfully generated an NPC catalyst with embedded Co in a one-step process; the catalyst was highly active for the oxidation of alcohols to esters in base-free conditions.<sup>106</sup> Via the galvanic replacement reaction between the Co and Pd<sup>2+</sup> in solution, Co@Pd core-shell nanoparticles embedded in the NPC (Co@Pd/NC) were synthesized and showed superior catalytic hydrogenation activity towards nitroarenes.<sup>107</sup> However, the high cost of MOFs goes does not agree with the principles of green and sustainable chemistry. In this regard, the group of Clark *et al.* pioneered a simple and environmentally friendly methodology to obtain mesoporous Starbon materials from starch through three main steps: 1) formation of gel by heating starch in water; 2) exchange of water with a lower-surface-tension solvent at low temperature ( $\approx 5$  °C); and 3) carbonization of the resulting as-prepared porous gels or the gels after drying to achieve the final mesoporous carbons (Scheme 2).<sup>52</sup> This method avoids the use of templates and can be performed at a temperature of choice (200–1000 °C), producing a wide range of mesoporous carbons as excellent catalysts or catalyst supports.<sup>145,146</sup> The Starbon synthetic method is thought to extend the carbon precursors beyond "neutral" polysaccharides such as nitrogen-containing chitosan and offers a simple production of NPC materials that can be extensively utilized in catalytic hydrogenations and oxidations.

### 3. Catalytic hydrogenations by NPC based catalysts

In the use of nitrogen-containing carbon-supported Pd or Pt NP catalysts in heterogeneous hydrogenations, the introduction of N-doping cannot only change the physicochemical and electronic properties of the support, but can also serve as basic or coordination sites to stabilize the small metal NPs.<sup>13,147,148</sup> Nitrogen-doped porous carbon materials have been intensively studied as catalyst supports for various hydrogenations. In this section, the use of NPC-supported NPs as the catalysts for a wide range of catalytic hydrogenation reactions including the hydrogenation of nitroarene, vanillin, phenol, benzoic acid, unsaturated bonds such as C=C, C≡C, -CHO or C≡N and N-heterocycles is reviewed. Notably, inexpensive metals (*e.g.*, Fe, Co and Ni) have become the new trend considering the high cost and scarcity of noble metals



**Scheme 2** Production of mesoporous carbon by controllable pyrolysis of expanded starch. (Magnified pictures of starch in flour and mesoporous starch obtained from scanning electron microscopy (SEM) and TEM for starbon). Reproduced with permission from ref. 52. Copyright© 2006 WILEY-VCH Verlag GmbH & Co. KGaA, Weinheim.

(*e.g.*, Pd, Pt and Au). Thus, we will introduce the various hydrogenation reactions mainly based on the kinds of metal used. We stress NPC-based composite-supported catalysts and bimetallic catalysts to give guidance to the design of more active and multifunctional catalysts.

#### 3.1 Noble metal-based hydrogenations

Aromatic amines are key building blocks and central intermediates for the chemical, pharmaceutical and agrochemical industries.<sup>149,150</sup> Catalytic reduction of nitroarenes over noble metal-based catalysts has been frequently studied.<sup>107,151–153</sup> Therefore, increasing interest in the preparation of noble metal-supported catalysts on NPC materials and their applications in the catalytic hydrogenation of functionalized nitroarenes has been seen. In this respect, the nitrogen-containing biomolecule dopamine was tested as a carbon source, and a nitrogen-doped hollow carbon was prepared through hard-templating. This hollow carbon functioned as a nanoreactor with encapsulated Au or Pd for nitroarene hydrogenation in the presence of NaBH<sub>4</sub> as the reductant.<sup>111,125</sup> The encapsulated nanoparticles were rather stable without aggregation after several cycles of recycling, which

highlighted the importance of nanoconfinement rather than the effect of nitrogen doping. Later, the hydrothermal carbonization of poly(2-aminothiazole) produced a nitrogen- and sulfur-co-doped porous carbon that was used to deposit Au NPs. The resulting catalyst was tested for nitroarene hydrogenation in the presence of  $\text{NaBH}_4$  or  $\text{H}_2$  as the reductant.<sup>109</sup> These works were just a test of the application of a novel support, and the actual effects of nitrogen were not noted. However, the intrinsic interaction between nitrogen and metal indeed matters significantly. The positive effect of nitrogen-metal interaction on catalytic hydrogenation because was elaborated in an early work by Wang and coworkers, who employed a  $\text{Pd}@mpg\text{-C}_3\text{N}_4$  catalyst in the hydrogenation of phenol.<sup>13</sup> The introduction of nitrogen atoms in the carbon framework changes the electronic properties of the support and provides coordination sites to stabilize the supported Pd NPs, which in turn greatly increase the reactivity and stability of the catalyst. For more works on metal NPs supported on  $\text{C}_3\text{N}_4$  in selective hydrogenations and oxidations, we suggest that the reader refer to a recent published review by the Wang group.<sup>154</sup> Since then, the use of nitrogen-doped porous carbon-supported metal catalysts in heterogeneous catalytic reactions has attracted intensive attention, and great progress was observed in recent years.

Using a post-treatment method with melamine as the nitrogen source, NPC materials (NAC-600, NAC-700, and NAC-800) were obtained through the heat treatments of mixtures of commercially available active carbon and melamine at the corresponding temperatures. All the  $\text{Pd}@NAC\text{-}T$  samples showed higher activity than  $\text{Pd}@AC$ , while  $\text{Pd}@NAC\text{-}800$  demonstrated the highest catalytic activity in the hydrogenation of nitroarenes in  $\text{H}_2$  atmosphere.<sup>40</sup> This result was attributed to the fact that the N species stabilized the Pd NPs and prevented their aggregation. At the same time, the N species accelerated the hydrogenation reaction. Further investigations found that the increased content of pyridinic and graphitic-type quaternary N in the NAC along with the increase in pyrolysis temperature were responsible for the high activity of  $\text{Pd}@NAC\text{-}800$ .<sup>40</sup>

Vanillin (4-hydroxy-3-methoxybenzaldehyde), a common component of pyrolysis oil, can be effectively hydrogenated into 2-methoxy-4-methylphenol, which is a potential future biofuel.<sup>43</sup> A pioneering work of vanillin hydrodeoxygenation was performed by Resasco *et al.*, who employed  $\text{Pd}@SWNT\text{-}SiO_2$  as an active catalyst in a water/oil emulsion and demonstrated enhanced catalytic performance.<sup>155</sup> Taking vanillin hydrodeoxygenation as a model reaction, Wang's group initially tested a nitrogen-doped porous carbon in the reaction as a highly active support for Pd NPs ( $\text{Pd}@CN_{0.132}$ ).<sup>43</sup> Typically, the dicyanamide-containing ionic liquid 3-methyl-1-butylpyridinedicyanamide was chosen as the NPC precursor, and 12 nm  $\text{SiO}_2$  nanoparticles was the hard template. After carbonization at 900 °C for 1 h followed by the removal of the silica template, a nitrogen-doped porous carbon was obtained. The as-obtained NPC holds a nitrogen content as high as 12 wt%, resulting in the stable anchoring of highly

dispersed Pd NPs with an average size of 4.1 nm (Fig. 3). When tested in the catalytic hydrodeoxygenation of vanillin, a greatly enhanced activity towards the targeted product 2-methoxy-4-methylphenol was observed compared with the  $\text{Pd}@SWNT\text{-}SiO_2$  catalyst under the same conditions (entries 1 and 2 in Table 1). It is notable that even better activity was observed when green and environmentally friendly water was used alone as the solvent (entry 3 in Table 1). All the tested commercially available supported Pd catalysts showed inferior activities compared to  $\text{Pd}@CN_{0.132}$  (entries 4–8 in Table 1). The catalyst was reused several times without losing activity and Pd leaching, which is promising for practical applications. The high catalytic performance was attributed to the special structure of the catalytic N-doped carbon-metal heterojunction, which leads not only to a very stable and uniform dispersion of Pd NPs, but also additional electronic activation of the metal NPs. Furthermore, the introduction of nitrogen in the carbon skeleton may greatly improve the hydrophilicity of the catalyst. This may be another major factor in promoting the high performance. The idea that the increased hydrophilicity of the catalyst could enhance its reaction activity was further evidenced by many other studies.<sup>156–158</sup> Following this work, a palladium-based ternary catalyst ( $\text{Pd}/\text{TiO}_2@\text{N-C}$ ) with two types of active sites was also applied in the hydrodeoxygenation of vanillin.<sup>159</sup> Notably, naturally available formic acid was used as the hydrogen source and was first decomposed at the  $\text{Pd}/\text{TiO}_2$  sites in  $\text{Pd}/\text{TiO}_2@\text{N-C}$ . Afterwards, the produced hydrogen was activated by the  $\text{Pd}/\text{N-C}$  sites, achieving full hydrogenation of vanillin into 2-methoxy-4-methylphenol as the sole product. The strategy for catalyst design of combining individual catalytic phases might open an alternative route for designing and developing catalysts for wide applications.

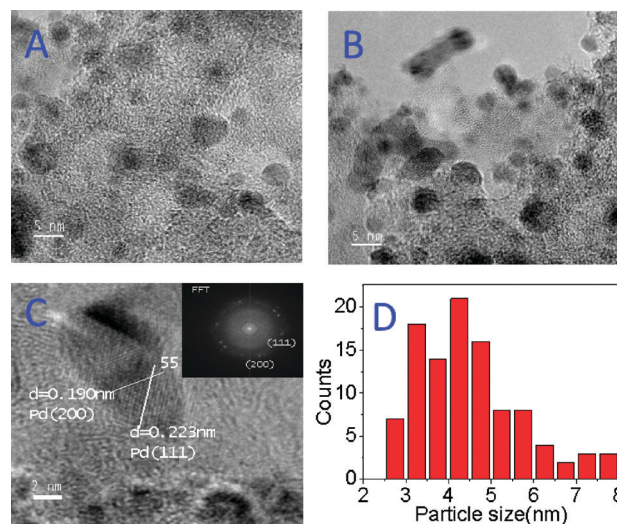


Fig. 3 HRTEM images showing A) and B) the distribution of the Pd NPs; C) the lattice fringes of the exposed Pd NPs (inset shows the corresponding FFT image); D) particle size distribution of deposited Pd NPs of  $\text{Pd}@CN_{0.132}$ . Reproduced with permission from ref. 43. Copyright© 2012 American Chemical Society.

**Table 1** Catalytic results for different catalysts Reproduced with permission from ref. 43. Copyright© 2012 American Chemical Society

Entry	Catalyst	Solvent	Conv. (%)	Selectivity <sup>a</sup> (%)	
				B	C
1 <sup>b</sup>	Pd@SWNT-SiO <sub>2</sub>	Water and decalin	85	53	47
2 <sup>c</sup>	Pd@CN <sub>0.132</sub>	Water and decalin	100	—	93
3	Pd@CN <sub>0.132</sub>	Water	100	—	100
4	Pd@C	Water	98	26	74
5	Pd@TiO <sub>2</sub>	Water	98	79	21
6 <sup>d</sup>	Pd@MgO	Water	28	32	—
7	Pd@CeO <sub>2</sub>	Water	88	86	14
8	Pd@γ-Al <sub>2</sub> O <sub>3</sub>	Water	95	31	69
9 <sup>e</sup>	Pd@CN <sub>0.132</sub>	Water	98	—	100

<sup>a</sup> B is the hydrogenation product, 4-hydroxymethyl-2-methoxyphenol, and C is the hydrogenation/hydrogenolysis product, 2-methoxy-4-methylphenol. <sup>b</sup> 1:1 (v/v) water/decalin; data taken from ref. 155. <sup>c</sup> 1:1 (v/v) water/decalin. <sup>d</sup> Other byproducts were unidentified. <sup>e</sup> S/C = 1000, H<sub>2</sub> pressure 1.0 MPa, 150 °C, 6 h.

NPC materials-supported Pd catalysts have also demonstrated activities in phenol hydrogenation to cyclohexanone, which is an important intermediate in the production of nylon 6 and nylon 66 in the chemical industry.<sup>24,110</sup> To investigate the effect of nitrogen doping on the resulting catalysts and their catalytic performance in phenol hydrogenation, Li *et al.* employed NH<sub>3</sub> or melamine as the nitrogen source to dope nitrogen in commercially available ordered mesoporous carbons. They achieved nitrogen loadings as high as 8.6 wt% while preserving the mesoporous structure. The N-doped carbons were used as supports to immobilize small-sized Pd NPs; the catalyst with ultrasmall (about 1.2 nm) Pd NPs gave the best reaction activity and selectivity under mild conditions.<sup>24</sup> It was experimentally revealed that the doped nitrogen not only dispersed and stabilized the small-sized Pd NPs, but also enhanced the catalytic hydrogenation activity and selectivity through weak interaction with the phenol molecule, which further confirmed the conclusion drawn by Wang's group.<sup>13</sup> A further work was reported by Wang and co-workers, who employed eight kinds of N-containing ILs (four pyridinium ILs and four imidazolium ILs) as the NPC precursors. They obtained a series of NPC materials with bulk nitrogen doping contents ranging from 9.5 wt% to 14.81 wt%, and the resulted NPC materials were deposited with Pd NPs to produce a series of Pd supported catalysts. Then a detailed investigation of the influence of the nitrogen heteroatom on the catalytic performance in phenol hydrogenation over the Pd supported catalysts was conducted.<sup>110</sup> The results showed that the percentage of Pd<sup>0</sup> was a key factor in controlling the catalytic performance. However, no clear conclusion about the relationship between IL-derived carbon and catalytic activity was suggested.

The search for a highly active Pd catalyst supported on NPC has never stopped, and the careful fabrication of NPC support is of essential importance. Recently, the Wang group

prepared a novel NPC with a nitrogen content of ~7 wt% *via* the hydrothermal treatment of glucosamine hydrochloride followed by heat treatment.<sup>128</sup> The produced supported Pd catalyst (Pd@CN) demonstrated an enhanced activity compared to Pd@CN<sub>0.132</sub> (a highly active Pd catalyst supported on an IL-derived NPC material in vanillin hydrogenation)<sup>43</sup> and an activity nine-times higher than that of commercial Pd@AC in the selective hydrogenation of benzoic acids (BA) to cyclohexane carboxylic acid (an important organic intermediate for the synthesis of pharmaceuticals such as a satrienin).<sup>160</sup> However, this was only a demonstration of the application of a novel NPC material in a new reaction, and further investigation is required to determine the reasons for the performance enhancement. There is no doubt that the introduced nitrogen heteroatom in the carbon skeleton may be the key point. The introduced nitrogen atom in the carbon framework may help to improve the reaction performance in the following ways: 1) the nitrogen sites may provide anchoring sites for metal particles, leading to a good dispersion of the catalyst;<sup>24,43</sup> 2) the electronegative property of the nitrogen sites may increase the electron density of the metal particle, thus keeping the metal in the metallic state during reactions;<sup>110</sup> and 3) the nitrogen sites may facilitate the absorption of reactant.<sup>13,53</sup>

As a test of the possible advantages brought by the introduction of nitrogen mentioned above, various kinds of NPC materials were employed as supports for anchoring finely dispersed Pd or Pt NPs. These materials offered nice activities in the selective hydrogenation of unsaturated bonds such as C=C,<sup>53,65,79,137,147</sup> -CHO (ref. 148 and 161) and N-heterocycles.<sup>162</sup> Interestingly, another “disadvantageous” property was found by the Nagashima group. They found that the NPC support functions to be a heterogeneous poisoning agent in (Z)-selective partial hydrogenation of internal alkynes and selective hydrogenation of substituted nitroarenes with reducible functional groups, respectively.<sup>163,164</sup> It is also notable that NPC materials are recommended for hybridization with other kinds of supports such as basic MgO to form a CN@MgO nanocomposites (Fig. 4) due to the bifunctional property obtained by combining the nitrogen functionalities, hydrophilicity and stability of NPC with the basicity of MgO.<sup>65</sup> The resulting Pd/CN@MgO served as a bifunctional catalyst with high catalytic activity towards the tandem aldol condensation-hydrogenation reaction of furfural with acetone in a one-pot reactor. However, this high activity was not comparable when a physical mixture of Pd@CN and Pd@MgO catalysts was used. Therefore, the catalyst design strategy provides a new method for the construction of metal-supported bi/multi-functional catalysts based on NPC materials for a wide range of applications.

It is also notable that bimetallic metals supported on NPC catalysts often produced performance enhancements.<sup>165–167</sup> Although very limited works have been done,<sup>25,26</sup> intensive studies on this topic can be expected. One example is bimetallic Au–Pd core-shell NPs trapped in an N-doped carbon (Au–Pd@N-carbon) catalyst fabricated *via* a HTC-PILs strategy

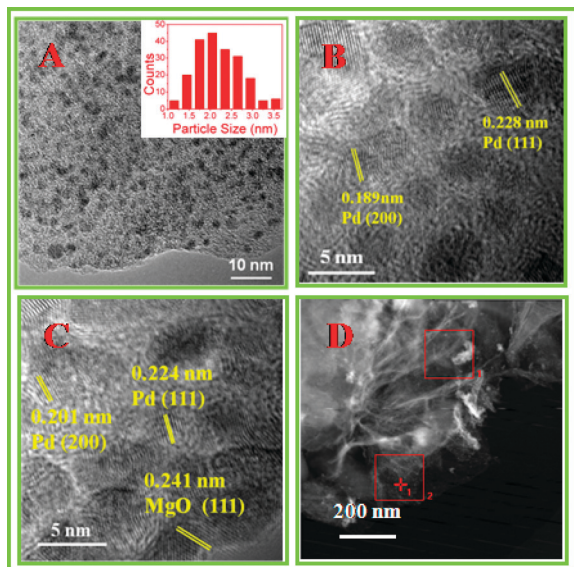


**Fig. 4** (A) HRTEM image showing the uniform distribution of Pd NPs with the particle size distribution of Pd NPs for ~200 particles of the Pd/CN@MgO nanocomposite (in the inset); (B) HRTEM image displaying the crystal planes of the surface Pd NPs; (C) HRTEM image clearly showing the amorphous morphology of the carbon coating with a uniform distribution of Pd NPs (NPs); (D) an STEM HAADF image of Pd/CN@MgO. Reproduced with permission from ref. 65. Copyright© 2014 The Royal Society of Chemistry.

by the Wang group. This catalyst was applied in heterogeneous hydrogenations.<sup>25</sup> Interestingly, the originally designed role of the PILs was to effectively stabilize the primary carbon NPs formed by HTC; however, they were further successfully coupled with PdCl<sub>2</sub> and HAuCl<sub>4</sub> as metal sources, with fructose serving both as carbon source and reducing agent, producing novel porous Au–Pd@N-carbon nano hybrids ( $S_{\text{BET}}$  up to 255 m<sup>2</sup> g<sup>-1</sup>). When used for the selective semi-hydrogenation of phenylacetylene, the as-prepared Au–Pd@N-carbon was more active than the single metal Pd@N-carbon, whereas 2.1% Au@N-carbon was inactive. These results revealed that the Au–Pd core-shell configuration had a positive influence on catalytic activity. It is hypothesized that the Au core may act as an electronic promoter for the Pd shell, which is the origin for the higher activity of the Au–Pd@N-carbon catalyst.<sup>25</sup> In addition, this catalyst could be recycled over 40 times without any apparent loss in activity (Fig. 5).

In another contribution by the Wang group, finely dispersed RuPd alloy NPs (average size = 3.6 nm) supported on nitrogen-doped carbon (RuPd/CN)<sup>26</sup> demonstrated much greater activity than a Pd@CN catalyst in BA hydrogenation.<sup>128</sup> High-resolution scanning transmission electron microscopy (STEM) analysis of the deposited NPs demonstrated the formation of atomic-level RuPd alloy (Fig. 6). XPS analysis revealed that the increased activity of RuPd/CN comes from the modulated electronic status of both Ru and Pd as a result of alloy formation; the Pd promoted the reduction of Ru<sup>n+</sup> with increased Ru<sup>0</sup>/Ru<sup>n+</sup> ratio, explaining the enhanced performance. Through first-principle studies of the

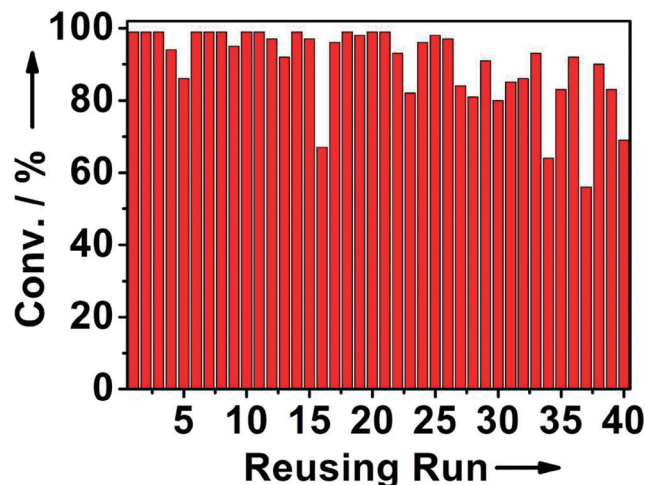


**Fig. 5** The reuse tests of 0.95% Au-1.1% Pd@N-carbon for phenylacetylene hydrogenation. Reproduced with permission from ref. 25. Copyright© 2013 WILEY-VCH Verlag GmbH & Co. KGaA, Weinheim.

adsorption modes of BA, particularly the configuration of the carboxyl group (Fig. 7), the reason for the superior selectivity (>99%) towards benzene ring hydrogenation was revealed by comparing the thermodynamics of hydrogenation and dissociation of the carboxyl group. In water solvent, the COOH H atom of BA, which chemisorbed on Ru and RuPd catalysts, dissolves into water spontaneously, meaning that the COOH group of BA is more likely to release an H atom than to receive one. Furthermore, the authors calculated the respective thermodynamics of COOH dissociation and hydrogenation on Pd, Ru and RuPd under vacuum. The positive COOH hydrogenation and dissociation energies for Pd implied that COOH tends to maintain itself since the surface H atoms from dissociated H<sub>2</sub> molecules prefer to stay on the surface rather than bind to COOH, and the dissociation of COOH is thermodynamically unfavorable at low temperatures. When it

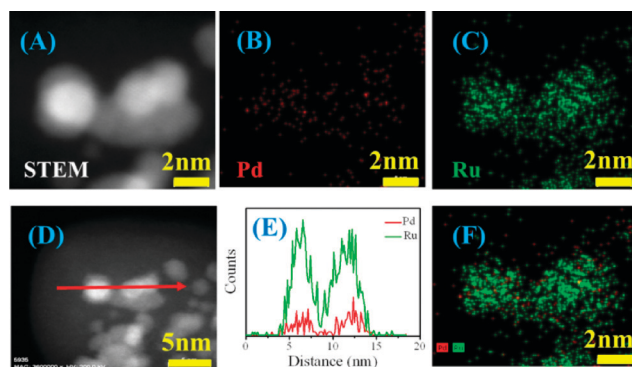


**Fig. 6** (A) HAADF-STEM image. (B) Pd-L and (C) Ru-L STEM-EDX maps obtained from a group of RuPd NPs of RuPd/CN. (D) Reconstructed overlay images of the maps shown in panels B and C: red, Pd; green, Ru. (E) Compositional line profiles of Pd and Ru for the RuPd NPs recorded along the arrow shown in the STEM image (D). Reproduced with permission from ref. 26. Copyright© 2015 American Chemical Society.

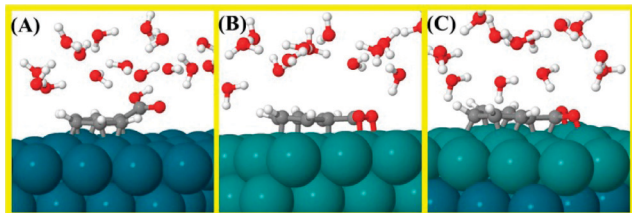


Fig. 7 Optimized adsorption modes of BA in water on (A) Pd, (B) Ru, and (C) RuPd catalysts. Color code: dark green, Pd; light green, Ru; gray, C; red, O; white, H. Reproduced with permission from ref. 26. Copyright© 2015 American Chemical Society.

comes to Ru and RuPd, positive COOH hydrogenation energies and negative dissociation energies were obtained, indicating that H thermodynamically dissociates from COOH, resulting in the binding of two O atoms to the catalyst surface. The above results fully explain the thermodynamically unfavorable hydrogenation of COOH.

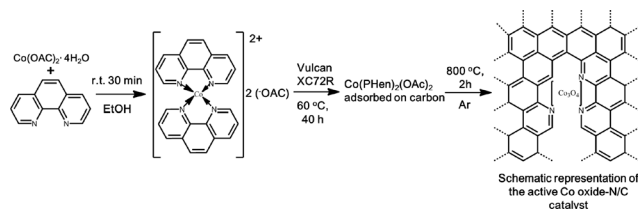
### 3.2 Non-noble metal-based hydrogenations

Though excellent catalytic hydrogenation performance was observed by employing noble metal catalysts, the high cost and scarcity of noble metals inspired researchers to develop inexpensive metal (e.g., Fe, Co, Ni) or metal-free catalysts as alternatives, with relatively low activity being the obstacle. Thus, Fe, Co and Ni in the metallic or oxidized forms were supported on NPC materials and demonstrated activity in the selective hydrogenations of nitroarenes<sup>27–30,95,98,127,168,169</sup> and nitriles.<sup>144</sup> The use of metal-free NPC materials in the catalytic reduction of 4-nitrophenol to 4-aminophenol seems more exciting.<sup>168,170</sup> Although the applications in hydrogenations are limited to very narrow areas, the desire to expand their uses to other catalytic applications studied in the noble metal-catalyzed hydrogenation reactions remains.

Valverde and coworkers conducted a detailed investigation into the impact of the nitrogen doping of carbon nanospheres on the nickel-catalyzed hydrogenation of butyronitrile. This was a relatively early research work on inexpensive metals supported on nitrogen-doped carbon in heterogeneous hydrogenations, although the carbons were all nonporous.<sup>144</sup> The undoped and nitrogen-doped nanospheres were prepared *via* the direct thermal pyrolysis of benzene, aniline or nitrobenzene at 1223 K for 2 h. After the deposition of nickel NPs, the obtained catalysts were tested in the gas-phase hydrogenation of butyronitrile. There were two interesting conclusions regarding the influence of nitrogen: 1) the introduced nitrogen, essentially in its quaternary form, led to an electron-enriched carbon surface, promoting the mobility of the metal and subsequent sintering; and 2) those larger particles deposited on the essentially quaternary nitrogen-doped surfaces delivered higher reaction rates by weakening the adsorption strength of the –CN group, thus making it easier to hydrogenate. Of course, the conclusion that the nitrogen atom (essentially quaternary nitrogen) demonstrated to be negative in stabilizing metal particles is in disagreement

with the widely accepted one that nitrogen helps stabilize deposited metal particles. This might be explained by the lack of pores where the metal particles are accessible to the nitrogen functionalities. The controllable synthesis of a series of NPC materials with adjustable nitrogen content or nitrogen type without changing the carbon precursor may be more reasonable.

Replacing the use of noble metals in the hydrogenation of nitroarenes with inexpensive metals, particularly Fe or Co hybridized with NPC, has witnessed a great breakthrough in this area,<sup>27,30,95,98</sup> and progress has also been made in developing Ni-based catalysts.<sup>127,168</sup> Inspired by the idea of preparing novel heterogeneous nanostructured catalysts from defined homogeneous organometallic complexes, the Beller group prepared a variety of Co oxide-N/C catalysts from different cobalt precursors and nitrogen ligands by adsorbing a solution of the respective cobalt complex onto commercially available carbon (Vulcan XC72R) and subsequent pyrolysis under inert conditions (Scheme 3).<sup>95</sup> The various organic nitrogen ligands not only controlled the resulting cobalt particle size, but also acted as nitrogen sources for obtaining nitrogen-doped carbon layers. The results showed that the most active catalyst employed 1,10-phenanthroline (L1) as the nitrogen ligand and possessed a wide dispersion and apparent agglomeration of particles (with particles larger than 800 nm). However, the less-reactive catalyst using 2,2':6',2''-terpyridine (L2) as the ligand had well-defined particles that rarely exceeded 2–10 nm. With these strange observations, the authors conducted XPS analysis of the catalysts. They found that the N1s XPS spectra of the active catalyst showed a new binding-energy peak at 399.0 eV, which can be attributed to a pyridine-type nitrogen bound to Co. Therefore, the authors concluded that the high activity was attributed to coordination of heterogeneous nitrogen with the formed Co<sub>3</sub>O<sub>4</sub>, regardless of the size of the Co<sub>3</sub>O<sub>4</sub> particles. The general scope of the present active catalyst was demonstrated in the reduction of more than 30 functionalized nitroarenes. It tolerates numerous other reducible functional groups and can be reused several times without loss of activity. Later, the same group changed cobalt salt to iron salt for the preparation of a Fe<sub>2</sub>O<sub>3</sub>-N/C catalyst for the same investigation of nitroarene hydrogenation.<sup>27</sup> This catalyst was demonstrated to be less active than the Co-based one reported elsewhere.<sup>95</sup>



Scheme 3 Synthesis of an active cobalt oxide-nitrogen/carbon catalyst by pyrolyzing a cobalt(II) acetate-phenanthroline complex on carbon. r.t. = room temperature. Reproduced with permission from ref. 95. Copyright© 2013 Macmillan Publishers Limited.

Although it showed inferior activity, by increasing the content of  $\text{Fe}_2\text{O}_3\text{-N/C}$  (4.5 mol% Fe) and the reaction temperature (120 °C),  $\text{Fe}_2\text{O}_3\text{-N/C}$  was able to selectively hydrogenate more than 40 kinds of structurally diverse and functionalized nitroarenes to anilines, which are important feedstocks and key intermediates for pharmaceuticals, agrochemicals and polymers.<sup>29</sup> This time, the authors demonstrated that particular  $\text{FeN}_x$  centers formed in a narrow range of pyrolysis temperatures around 800 °C govern the unique catalytic activity, while the size of the iron oxide particles seems to play a minor role.<sup>27</sup> After replacing  $\text{H}_2$  with formic acid as the hydrogen donor, the  $\text{Fe}_2\text{O}_3\text{-N/C}$  catalyst also exhibited remarkable activity for the activation of formic acid in the transfer hydrogenation of nitroarenes to anilines with unique selectivity.<sup>98</sup>

Even though great progress in cobalt-catalyzed nitroarene hydrogenation has been achieved by the Beller group, the high cost of the added nitrogen ligand and the relatively harsh reaction conditions (5 MPa  $\text{H}_2$ ) in their catalytic system leaves the desire for more easily accessible Co catalysts that can be handled in milder conditions. Furthermore, the transformation of the Co species in the hydrogenation reactions requires detailed investigation. As a response to this, an earth-abundant  $\text{CoO}_x\text{@N}$ -doped carbon nanotube catalyst (denoted as  $\text{CoO}_x\text{@NCNTs}$ ) was fabricated *via* the efficient thermal condensation of naturally available D-glucosamine hydrochloride, melamine, and  $\text{Co}(\text{NO}_3)_2\cdot 6\text{H}_2\text{O}$  at 900 °C by the Wang group. This catalyst exhibited excellent catalytic activity and perfect chemoselectivity (>99%) for a wide range of substituted nitroarenes (21 examples) under relatively mild conditions (3 MPa  $\text{H}_2$ ).<sup>30</sup> The hybrids were characterized as nitrogen-doped multiwalled carbon nanotubes with lengths of several micrometers and thicknesses of 50–100 nm with finely dispersed nanoparticles of a mean size of 12.9 nm (Fig. 8a–b). The NPs were either in the form of crystalline  $\text{Co}_3\text{O}_4$

(Fig. 8c) or  $\text{Co}^0$  protected by nitrogen-doped graphene layers (Fig. 8d). Although these catalysts exhibited high activity, recycling experiments showed that Co leaching took place.  $\text{Co}_3\text{O}_4$  was readily converted to  $\text{CoO}$ , and  $\text{CoO}$  was also transformed to  $\text{Co}^0$ . These transformations led to a decrease in activity after recycling. However, this phenomenon was not mentioned in the previous work by the Beller group.<sup>95</sup> The unexpected stability of  $\text{Co}^0$  thus inspired the authors to investigate the catalyst in detail, and catalyst consisting of  $\text{Co}^0$  covered with nitrogen-doped graphene layers (denoted as  $\text{Co}^0\text{@NCNTs}$ ) was easily obtained by the acid treatment of  $\text{CoO}_x\text{@NCNTs}$ . When applied to nitrobenzene hydrogenation, this catalyst shows even better performance than  $\text{CoO}_x\text{@NCNTs}$  and can be recycled up to five times with insignificant loss in activity, verifying the improved resistance of  $\text{Co}^0$  against oxidation with the aid of nitrogen-doped graphene layers. This interesting observation further encouraged the authors to carry out density functional theory calculations. The results indicated that the  $\text{Co}^0$  and N in the hybrids can simultaneously tune the inert graphene layer to be active in  $\text{H}_2$  activation by lowering its dissociation energy, suggesting that the cooperative effect between  $\text{Co}^0$  species and nitrogen was responsible for the high activity. The synthetic strategy provides a versatile platform to fabricate a series of functional non-noble metal@NPC hybrids, which also showed good performance for diverse applications. For example, by simply changing the cobalt precursor to  $\text{Co}(\text{Ac})_2\cdot 4\text{H}_2\text{O}$ , the resulting Co catalyst was shown to be highly active in the selective hydrogenation of 2,3,5-trimethylbenzoquinone.<sup>143</sup> By decreasing the calcination temperature to 800 °C, a flake-like  $\text{CoO}_x\text{@CN}$  hybrid was fabricated, which was demonstrated to be a superior bifunctional electrocatalyst for hydrogen and oxygen evolution.<sup>171</sup> This synthesis also enables the change of Co to other non-noble metals such as Ni, which have further expanded the present fabrication system for a wide range of catalytic reactions.<sup>142</sup>

Besides the intensive use of NPC materials as catalyst supports in catalytic hydrogenations, they can also be directly employed as catalysts in the metal-free catalytic hydrogenation reactions. In a related work, the Chen group introduced metal-free nitrogen-doped graphene (NG) for the catalytic reduction of 4-nitrophenol to 4-aminophenol; the catalyst achieved high activity in the presence of  $\text{NaBH}_4$  as the reductant.<sup>170</sup> When comparison experiments were performed employing nitrogen-doped graphite, pristine graphite, GO and reduced GO as the catalysts, only the nitrogen-doped graphite was catalytically active, and its activity was much lower than that of NG. Interestingly, the present reaction mediated by NG follows pseudo-zero-order kinetics, which is completely different from all of the reported pseudo-first-order reactions catalyzed by metal NPs. Therefore, considering only the adsorption of nitrophenol on the surface of NG, detailed investigations including *in situ* Fourier Transform Infrared Spectroscopy (FTIR) and density functional theory (DFT) were performed. The results suggested that nitrophenol ions tend to interact with NG *via* the O atom of the

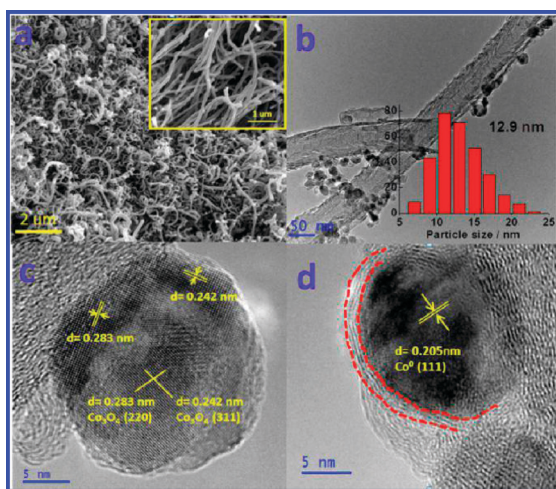


**Fig. 8** Representative SEM image (a), TEM image (b), and HRTEM images (c, d) of  $\text{CoO}_x\text{@NCNTs}$ . Inset (a) is magnification of the SEM image, and inset (b) is the metal particle size distribution histogram. Reproduced with permission from ref. 30. Copyright© 2015 American Chemical Society.

hydroxyl group, and only the carbon atoms next to the doped N atoms can be activated and catch the nitrophenol ions due to its weakened conjugation and higher positive charge density. Further, all of the pyridinic, pyrrolic, amine and graphitic nitrogen species have good performance for nitrophenol adsorption, and the nitro groups of the adsorbed nitrophenol ions are all activated. That is why nitrogen doping can have such a positive effect on promoting the catalytic performance. Despite this fantastic discovery, the tedious synthetic process of NG and the use of toxic chemicals limited its wide use to some extent. Thus, the sustainable synthesis of catalytically active metal-free alternative NPC materials is highly desired. To this end, employing sustainable chicken feathers as both the nitrogen and carbon precursor, the same group prepared nitrogen-containing carbon nanotubes (N-CNTs) that demonstrated even higher activity than NG in the metal-free catalytic reduction of 4-nitrophenol to 4-aminophenol.<sup>168</sup>

## 4. Catalytic oxidation using NPC-based catalysts

Oxidation reactions, another important transformation for the industrial production of a wide range of chemicals and reactive intermediates, have also seen great development by using NPC-based catalysts. In this section, we introduce catalytic oxidation reactions based on the kinds of catalysts used: NPC-supported noble metal catalysts and non-noble metal ones along with NPC materials alone as metal-free catalysts. Noble metals such as Pt, Pd, Au and Ru supported on NPC materials have been tested in a wide range of oxidation reactions like the oxidation of methane, CO, benzoic alcohols, hydrocarbons, glycerol and phenol. By supporting non-noble Co oxide on a NPC support, the Beller group observed superior catalytic activity for the selective oxidation of alcohols to esters.<sup>94</sup> This inspired intensive interest in uncovering their ability in a wide range of oxidation reactions, including the epoxidation of alkenes, synthesis of nitriles from the oxidation of alcohols with ammonia, and oxidative dehydrogenation of N-heterocycles. Notably, the mechanisms of oxidation reactions often involve free radicals, and oxidation reactions can even take place in the absence of catalysts *via* non-catalytic autoxidation.<sup>104</sup> Therefore, the induced defects and charge redistribution in the carbon structures due to nitrogen doping may even enable NPC materials as metal-free catalysts in the oxidation reactions. Not surprisingly, even wider ranges of applications have been explored, including the oxidation of SO<sub>2</sub> to SO<sub>3</sub> or H<sub>2</sub>SO<sub>4</sub>, H<sub>2</sub>S to sulfur, and NO to NO<sub>2</sub> as well as liquid-phase oxidation reactions such as the oxidation of alcohols (aromatic alcohols and aliphatic alcohols) and C–H bonds (cyclohexane, ethylbenzene, cumene and other hydrocarbons) and the epoxidation of alkenes (styrene, *trans*-stilbene). Considering the high cost of noble metals and easy leaching of non-noble metals in heterogeneous oxidations, metal-free NPC catalysts demonstrate great potential

for various oxidations in the future, although limited activity may be the obstacle.

### 4.1 Metal-based oxidations

As is in the case of hydrogenation, the advantages of nitrogen species in NPC for anchoring, stabilizing and coordinating with the deposited metal NPs have further inspired researchers to perform a wide range heterogeneous catalytic oxidation reactions. Noble metals such as Pt, Pd, Au and Ru supported with NPC materials were tested in industrially related oxidation reactions such as the oxidation of methane,<sup>105</sup> CO,<sup>116,172</sup> benzoic alcohols, hydrocarbons,<sup>31</sup> glycerol<sup>121</sup> and phenol.<sup>118</sup> Although non-noble metals supported on NPC catalysts saw very limited developments in this area,<sup>117,126</sup> a great breakthrough was made by Beller group with the creation of Co- and Fe-based nanocatalysts activated by nitrogen-doped graphene layers; these catalysts have been applied in various oxidations such as the direct oxidative esterification of alcohols,<sup>94,173</sup> epoxidation of alkenes,<sup>101</sup> synthesis of nitriles from the oxidation of alcohols with ammonia,<sup>103</sup> and oxidative dehydrogenation of N-heterocycles.<sup>100</sup> The non-noble metal-based systems are expected to further expand their areas of applications in oxidation reactions, and bimetallic metal-based catalysts are welcomed to improve performance in this area.<sup>167,174</sup> Table 2 gives a brief summarization of the state-of-the-art metal catalysts supported on NPC, which demonstrated diverse catalytic oxidation activities in various applications.

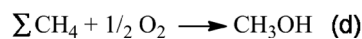
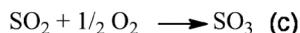
**4.1.1 Noble metal-based oxidations.** By mimicking the molecular Periana catalyst used in the low-temperature oxidation of methane to methanol by SO<sub>3</sub> in concentrated sulfuric acid (Scheme 4), the group of Ferdi Schüth developed a solid catalyst by coordinating a Pt<sup>2+</sup> species to a low-cost and naturally available nitrogen-rich NPC (derived from lobster exoskeleton).<sup>132</sup> This catalyst showed higher activity than the published Pt-CTF system,<sup>105</sup> but more pronounced deactivation was observed.<sup>132</sup> Although, the reasons for the high activity and loss of activity during recycling were not clear, this work may provide new insights for further targeted material development, which could bring catalytic methane utilization closer to technical feasibility.

The selective oxidation of organic compounds such as benzoic alcohols or hydrocarbons, a primary and essential inorganic transformation in industrial chemistry, has become a hot topic in the heterogeneous oxidations. The activities of noble metals supported by NPC materials have also been investigated, mainly for Pd-supported catalysts,<sup>31,115,175</sup> although Au supported on nitrogen-doped graphene was also studied.<sup>176</sup> The various studies demonstrated enhanced oxidation activity and catalyst stability by introducing nitrogen heteroatoms into the carbon structure. These enhancements were due to the increased metal–support interaction and better metal dispersion with the decrease in particle size. However, the turnover frequencies (TOFs) for alcohol oxidation were relatively low, largely restricting the wide application of

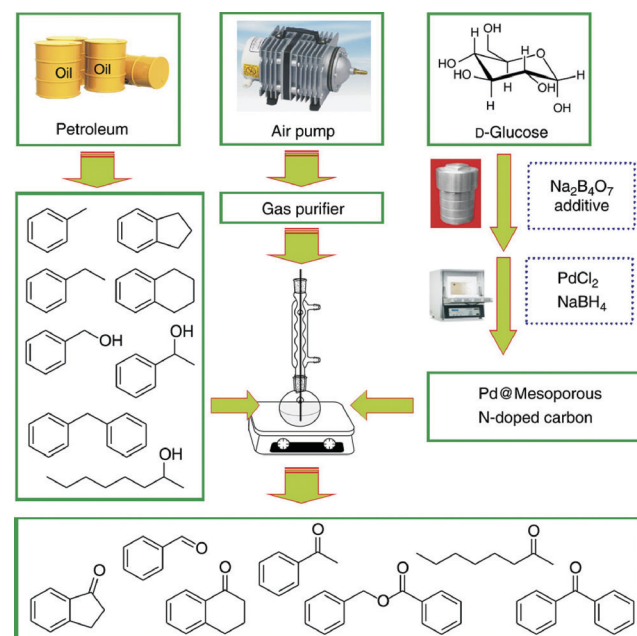
**Table 2** NPC-supported metal catalysts employed for various oxidation reactions

Catalyst	Temp. (°C)	Oxidant	Application	TOF (h <sup>-1</sup> )	Ref.
Pt@ExLOB	215	Oleum	Methane oxidation	1802	132
Pd@N-doped carbon	160	Oxygen (1 atm)	Benzyl alcohol oxidation	~210 000	31
Pd@PBFS	80	Oxygen (1 atm)	Benzyl alcohol oxidation	690	115
Pd/NCS or AuPd/NCS	120	Oxygen (1.5 atm)	Benzyl alcohol oxidation	43 000–65 000	175
Au/NG	70	Oxygen (1 atm)	Benzyl alcohol oxidation	~1	176
Pt/CNTs	60	Oxygen (1 atm)	Glycerol oxidation	459	80
Pt/N-MWCNTs	60	Oxygen (5 atm)	Glycerol oxidation	354	92
Pt/NCNTs	60	Oxygen (1 atm)	Glycerol oxidation	2592	121
Co <sub>3</sub> O <sub>4</sub> -N@C	60	Oxygen (1 atm)	Benzyl alcohol alcohols oxidative esterification	1.67	94
Co <sub>x</sub> O <sub>y</sub> -N/C	70	<i>tert</i> -BuOOH	Alkenes epoxidation	~1.25	101
Co <sub>x</sub> O <sub>y</sub> -N@C	100	Oxygen (10 atm)	HMF oxidation	~6.5	173
Co <sub>3</sub> O <sub>4</sub> -NGr/C or Fe <sub>2</sub> O <sub>3</sub> -NGr/C	130	O <sub>2</sub> and <i>t</i> -amylalcohol	Nitriles synthesis from alcohols	~1.3	103
FeO <sub>x</sub> @NGr-C	100	Air (20 atm)	N-heterocycles dehydrogenation	~46	100
Co <sub>3</sub> O <sub>4</sub> -NGr/C	60	Oxygen (1 atm)	N-heterocycles dehydrogenation	10	99
Co/N-HCS	110	Oxygen (1 atm)	Styrene oxidation	245	126
Co@C-N	25	Air (1 atm)	Alcohols oxidative esterification	~0.07	106

these catalysts.<sup>115,176,177</sup> Recently, the Wang group treated glucose hydrothermally in the presence of N-containing additives followed by carbonization at 550 °C in N<sub>2</sub>. They obtained an NPC constructed with ~20 nm carbon NPs, which functions as a support for constructing a highly active Pd catalysts for the solvent-free oxidation of alcohols (TOF of up to ~210 000) and hydrocarbons (TOF of up to 863; Fig. 9).<sup>31</sup> In contrast to the conclusion that the nitrogen species decrease the size of Pd, the Pd NPs observed on the nitrogen-doped carbon in this study had similar sizes to those on the nitrogen-free carbon support. This observation suggested that the nitrogen-doped carbon is the origin of the activity enhancement. On one hand, both the doped nitrogen atoms and the increased structural defects due to the incorporation of nitrogen in the carbon are expected to anchor substrates efficiently and lead to the enhancement substrate adsorption on the catalyst surface, which in principle could boost the oxidation process. On the other hand, the doped nitrogen atoms, especially those with lone pairs, might enhance the electron density of Pd<sup>0</sup>, thus promoting the oxidative addition of the O–H or C–H bond to the Pd<sup>0</sup> species, resulting in an increased reaction rate. It is also interesting to note that the introduction of an organic ligand, 2-acetylpyridine, could accelerate the heterogeneous Pd catalytic oxidation of indane. With the above observations, the present work presents a simple strategy to tune the oxidation activities of supported metal particles through the introduction of nitrogen-doped carbon materials or organic ligands.

**Scheme 4** Equations involved in the oxidation of methane by SO<sub>3</sub> in concentrated sulfuric acid.

Glycerol oxidation, an important reaction that produces valuable chemicals, was previously carried out in the presence of the basic additive NaOH,<sup>178</sup> which complicates the operation process and may lead to environmental pollution. Thus, it is desirable to replace traditional homogeneous bases with heterogeneous ones from the viewpoint of environmental protection and green chemistry. Considering the weak basic properties of NPC materials because of the introduction of nitrogen species in the carbon skeleton, NPC materials were employed as both supports for Pt NPs and heterogeneous basic additives for the base-free oxidation of glycerol.<sup>80,92,121</sup> Apart from the achieving basicity under base-free

**Fig. 9** Synthetic and catalytic strategy. The substrates and reactors used in the aerobic oxidation, the device for air production and the method for catalyst preparation. Reproduced with permission from ref. 31. Copyright © 2013 Macmillan Publishers Limited.

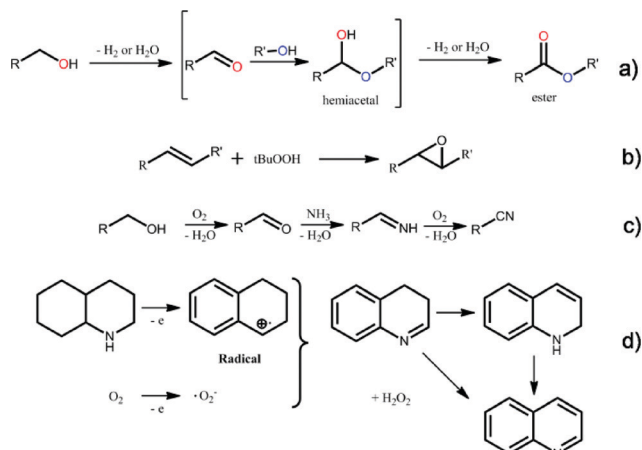
reaction conditions, enhanced reaction activity, higher selectivity towards glyceric acid and better reaction stability of the Pt catalysts were observed, and the nitrogen heteroatom played an important role.<sup>80,92</sup> Despite the widely documented conclusions that the doped nitrogen may improve the dispersion and durability of Pt NPs on carbons, the type of nitrogen functionality on the NCNTs that is responsible for anchoring metallic NPs remains unclear. By changing the content of Pt and the nitrogen content of the supporting NCNTs, Yu and coworkers demonstrated that the graphitic nitrogen species on NCNTs are primarily responsible for the enhanced catalytic oxidation activity of glycerol.<sup>121</sup> These insights are helpful in understanding the fundamentals of catalysis involving N-doped carbon materials as supports. Yet, continuous efforts towards this end are still needed in the future.

**4.1.2 Non-noble metal-based oxidations.** When it comes to heterogeneous oxidations based on NPC-supported non-noble metal catalysts, great contributions were made by the Beller group, who discovered Co- and Fe-based catalysts in 2013.<sup>27,95</sup> These two fantastic works illustrated the excellent activities of the two catalysts for the hydrogenation of nitroarenes. Nonetheless, they also happened to be excellent oxidation catalysts for the direct oxidative esterification of alcohols,<sup>94,173</sup> epoxidation of alkenes,<sup>101</sup> synthesis of nitriles from the oxidation of alcohols with ammonia,<sup>103</sup> and oxidative dehydrogenation of N-heterocycles.<sup>99,100</sup> Here, we introduce the Co- and Fe-based catalytic systems developed by the Beller group for various areas of oxidation; in addition, some limited works on the modified catalytic systems are discussed.<sup>106,117,126</sup>

The Beller group initially tested the activity of a  $\text{Co}_3\text{O}_4\text{-N@C}$  catalyst for the oxidation of alcohols to esters.<sup>94</sup> Esters are used as important building blocks in the chemical industry and are found in numerous pharmaceuticals, agro-

chemicals, fragrances, and polymers. Among the various synthetic protocols, the direct transformation of alcohols to esters constitutes an interesting alternative (Scheme 5a). Thus,  $\text{Co}_3\text{O}_4\text{-N@C}$  was first tested in this reaction with the addition of basic additives ( $\text{K}_2\text{CO}_3$  or  $\text{K}_3\text{PO}_4$ ) at temperatures of 60–120 °C for 24–30 h under atmospheric  $\text{O}_2$ , resulting in the synthesis of a series of structurally diverse esters (up to 64 examples) as well as other alkyl esters in good to excellent yields. The oxidative self-esterification of both aliphatic and aromatic alcohols was then demonstrated.<sup>94</sup> With the exciting results in the first test of using the  $\text{Co}_3\text{O}_4\text{-N@C}$  catalyst for oxidation, the Co-based catalyst was further applied to industrially relevant oxidations. One was the epoxidation of alkenes with *tert*-butyl hydroperoxide as the oxidant (Scheme 5b), which produced epoxides covering various aromatic and aliphatic epoxides with excellent selectivity and often high yields. In addition, this heterogeneous catalyst was shown to be useful for the oxidation of renewable olefins as well as vitamin and cholesterol derivatives.<sup>101</sup> The other one was the benign synthesis of nitriles, including all kinds of structurally diverse aryl, heterocyclic, allylic and aliphatic nitriles, from easily available alcohols using aqueous ammonia and molecular oxygen (Scheme 5c). Using this protocol, the renewable synthesis of adiponitrile, an important feedstock for the nylon 6,6 polymer, was achieved.<sup>103</sup> Notably, the Fe-based catalyst, which was less active in nitroarenes hydrogenation, also demonstrated similar activity in the synthesis of nitriles from alcohols and ammonia.<sup>103</sup> The catalytic oxidative dehydrogenation of N-heterocycles constitutes a fundamental process in organic synthesis, producing pharmaceuticals and other biologically active molecules. Only recently has the modified Fe activated by nitrogen-doped carbon layers developed by the Beller group seen application in this area (Scheme 5d), allowing for the green dehydrogenations of several N-heterocycles, including the synthesis of pharmaceutically relevant quinolines.<sup>100</sup> With the assistance of  $\text{K}_2\text{CO}_3$ ,  $\text{Co}_3\text{O}_4\text{-N@C}$  also achieved high activity in this reaction.<sup>99</sup>

The abovementioned examples are only limited oxidation reactions, and we believe that the applications of NPC materials will be further expanded to areas including CO oxidation, which was tested using a  $\text{Co}_3\text{O}_4$  catalyst supported by nitrogen-doped CNFs.<sup>117</sup> Notably, the catalytic activities in all the tested oxidation reactions originates from the specific interactions between Fe or Co with the nitrogen-doped carbon layers; more specifically, the activity is attributed to the coordination between Fe or Co with the nitrogen atoms in the carbon layers.<sup>27,95</sup> However, improvements still remain to be made. For example, a  $\text{Co@C-N}$  catalyst derived from the pyrolysis of a MOF ZIF-67 developed by Li and coworkers was successfully applied in more than 34 examples of base-free oxidative esterifications of alcohols under mild conditions;<sup>106</sup> these examples did not use the basic additives in the Co-based catalyst that were used by the Beller group.<sup>94</sup> Considering the high cost of the fabrication process of the current NPC-based non-noble metal catalysts used in oxidations, more easily accessible and renewable NPC-supporting



**Scheme 5** The various heterogeneous oxidation reactions catalyzed by NPC-supported Co or Fe catalysts: a) oxidative synthesis of esters from alcohols; b) epoxidation of alkenes with *tert*-butyl hydroperoxide; and c) general reaction pathway for the synthesis of nitriles from alcohols. d) The catalytic pathway for the dehydrogenation of N-heterocycles. Reproduced with permission from ref. 94, 100, 101 and 103. Copyright American Chemical Society, WILEY-VCH VerlagGmbH & Co. KGaA, Weinheim and Macmillan Publishers Limited.

non-noble metal catalysts are expected to be developed, and even greater catalytic activity for a wider range of oxidation systems is anticipated.

#### 4.2 Metal-free oxidations

Confronted with the problems of easy leaching and sintering of supported metal NPs in supported-metal catalysts, researchers thus have devoted their energy to the investigation

of metal-free alternatives. Recent reviews by Su *et al.* have highlighted the advantages and promising prospects of using metal-free nanocarbon catalysts for sustainable chemistry, particularly in the oxidation area.<sup>18,179</sup> Tremendous improvements in the catalytic activities of NPC-supported metal catalysts in the abovementioned hydrogenations and oxidations due to the incorporation of nitrogen atoms in the carbon supports have been demonstrated; thus, doping nitrogen atoms into the carbon skeletons is expected to be more

**Table 3** NPC catalysts employed in various metal-free oxidation reactions

Material	Nitrogen doping method	Nitrogen content (wt%)	Activity origin	Molecule for oxidation	Activity <sup>b</sup> (mmol g <sup>-1</sup> h <sup>-1</sup> )	Ref.
N-AC; N-ACF	Post treatment with DMF, NH <sub>3</sub> , DCD or urea	0.4–4.6	Pyridinic N	SO <sub>2</sub>	~85	83
NMC (N-mesoporous carbon)	Direct synthesis with melamine	4.3–11.9	Pyridinic N	H <sub>2</sub> S	~160 <sup>c</sup>	119
N@CFS	Direct synthesis from polyacrylonitrile	10.6–16.2	High graphitization	H <sub>2</sub> S	~10 <sup>c</sup>	108
N-CNTs; NCNTs/SiC	Direct synthesis with NH <sub>3</sub>	1.2–4.1	Nitrogen doping effect	H <sub>2</sub> S	~15–25 <sup>c</sup>	180, 181
N-AC	Post treatment with urea	0.82–1.65	Nitrogen doping effect	NO	—	82
NCM (N-carbon xerogel)	Post treatment with urea or melamine	2.0–5.3	Pyridinic and pyrrolic N	NO	30 <sup>d</sup>	120
NCNF	Posttreatment with NH <sub>3</sub>	3.21–5.21	Nitrogen doping	NO	—	75
NG	Post treatment with ammonium nitride	5–8 <sup>a</sup>	Enhanced electron transfer	Phenol	~1–4	84–86
NCNTs	Post treatment with melamine	0.75–0.8 <sup>a</sup>	Enhanced electron transfer	Phenol	~6	182
NG	Post treatment with urea or melamine	7.5–9.3	Nitrogen doping effect	Phenol	~6	183
NG (N-doped graphene)	Posttreatment with NH <sub>3</sub>	1.71–4.16	Graphitic N	Benzyl alcohol	~0.05	97
NCNTs	Direct synthesis with aniline	0.2–3.0	Enhanced electron transfer	Benzyl alcohol	~30	184
NCNTs	Direct synthesis with aniline	0.2–3.0	Enhanced electron transfer	Benzyl alcohol	~16	185
N-ADD (N-doped annealed nanodiamond)	Post treatment with imidazole or NH <sub>3</sub>	Up to 5.0	Pyridinic N	Benzyl alcohol	~9	33
N-AC (N-doped activated carbon)	Post treatment with NH <sub>3</sub>	Up to 5.3	Graphitic N	Benzyl alcohol	~0.3	55
NCNTs	Direct synthesis from aniline	4.5 <sup>a</sup>	Enhanced electron transfer	Cyclohexane	879	124
NCNTs	Direct synthesis from aniline	0.31–3.44 <sup>a</sup>	Enhanced electron transfer	Cumene	157.5	122
NCNTs	Direct synthesis from aniline	0.3–4.36	Enhanced electron transfer	Cyclohexene	620.1	104
NG	Direct synthesis from chitason	6.6	Carbon adjacent to nitrogen	Cyclooctane	~40–60	186
NG	Post treatment with acetonitrile	1.1–8.9	Carbon adjacent to graphitic nitrogen	Ethylbenzene	~4–20	32
NDC	Direct synthesis from melamine	4.4–11.9 <sup>a</sup>	Graphitic nitrogen	Ethylbenzene	~13	134
NG	Post treatment with hydrazine	3.54–6.35	Nitrogen doping effect	Aromatic and aliphatic C–H	~1–3	81
NOMC (N-doped mesoporous carbon)	Direct synthesis from <i>m</i> -aminophenol	0.9–3.3 <sup>a</sup>	Nitrogen doping effect	Ethylbenzene	144.6	136
NAC	Post treatment with NH <sub>3</sub> or NO	1.56–4.04	Pyridinic N	Xanthene	0.28 <sup>e</sup>	187
NG	Post treatment with NH <sub>3</sub>	0.42–1.29	Carbon adjacent to graphitic nitrogen	<i>trans</i> -Stilbene and styrene	~25	56
NOLC (N-doped onion-like carbon)	Post treatment with NH <sub>3</sub>	2.06–3.95 <sup>a</sup>	Carbon adjacent to graphitic nitrogen	Styrene	~35	76

<sup>a</sup> Atomic percent of nitrogen. <sup>b</sup> Reaction rate of substrate consumption normalized by catalyst mass. <sup>c</sup> Calculated from weight hourly space velocity (the mass of H<sub>2</sub>S feed per mass of NPC catalyst per hour) and corresponding conversion data. <sup>d</sup> Reaction rate of substrate consumption normalized by the surface area (mmol m<sup>-2</sup> h<sup>-1</sup>). <sup>e</sup> TOF (h<sup>-1</sup>) based on the number of surface pyridine-type N species.

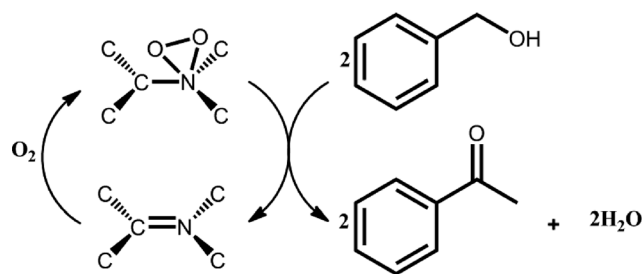
advantageous than using pure nanocarbons in catalytic oxidation reactions. Without the influence of the deposited metals, employing metal-free NPC materials as the catalysts may also enable better control of the active-site, more specifically, the specific nitrogen species. Indeed, metal-free NPC catalysts have been used in a wide range of oxidation reactions. In this section, a series of recent oxidation reactions including the gas-phase oxidations of  $\text{SO}_2$  to  $\text{SO}_3$  or  $\text{H}_2\text{SO}_4$ ,  $\text{H}_2\text{S}$  to sulfur, and  $\text{NO}$  to  $\text{NO}_2$  along with the liquid-phase oxidations of alcohols (aromatic alcohols and aliphatic alcohols) and C–H bonds (cyclohexane, ethylbenzene, cumene and other hydrocarbons) and the epoxidation of alkenes (styrene, *trans*-stilbene) are reviewed. Moreover, insights from mechanistic studies and active site discussions for related reactions are included. For clarity, the nitrogen doping methods, nitrogen contents of the employed NPC catalysts, the active centers and the reaction rates for the oxidation reactions are summarized in Table 3.

Atmospheric contamination is one of the most important environmental problems caused by progressive industrialization and threatens human health. Toxic gases such as  $\text{SO}_2$ ,  $\text{H}_2\text{S}$ ,  $\text{NO}$  and  $\text{CO}$  are frequently emitted into the atmosphere. With the increasing environmental awareness and implementation of more stringent emissions regulations, researchers have devoted their energies to controlling and reducing toxic gas emissions.<sup>188</sup> NPC materials have demonstrated potential in this field, particularly through metal-free catalytic oxidation, although  $\text{CO}$  oxidation remains in the theoretical stage.<sup>189</sup>

In very early works, the catalytic activities of NPC materials used as metal-free catalysts for  $\text{SO}_2$  oxidation were demonstrated, and enhanced catalytic performance was observed as a result of nitrogen doping.<sup>190,191</sup> However, the nature of the nitrogen species responsible for the enhanced activity remained unclear. In response to this issue, Cazorla-Amorós *et al.* synthesized a number of nitrogen-doped activated carbons (N-AC) and nitrogen-doped activated carbon fibres (N-ACF) with a wide range of nitrogen contents and different distributions of chemical species. When N-AC and N-ACF were applied in  $\text{SO}_2$  oxidation, the presence of N species at the surface increased the catalytic activity, and the pyridinic nitrogen species contributed the most to the activity enhancement.<sup>83</sup> From then on, NPC materials have been applied to the oxidation of  $\text{H}_2\text{S}$  to recover sulfur, an important process for the utilization of gasified products from many industrial processes. The group of Pham-Huu initially developed NCNTs for the efficient oxidation of  $\text{H}_2\text{S}$  to sulfur and obtained excellent activity along with high stability (more than 120 h) during testing at a relatively high space velocity ( $1.2 \text{ h}^{-1}$ ). The authors attributed this high stability to the active nitrogen sites embedded inside the carbon matrix, which were responsible for the formation of the activated oxygen species.<sup>180</sup> To further increase the catalytic activity, the NCNTs were macroscopically shaped on silicon carbide foam to improve the contact between the reactants and the catalyst.<sup>180,181</sup> However, there was no evidence of the exact active centers respon-

sible for the improved activity, although nitrogen indeed facilitates this improvement. A subsequent work by the same group employed nitrogen-doped carbon fibers (N@CFs) prepared by electrospinning for the same reaction and concluded that a synergic effect between the incorporated nitrogen species and a high graphitization degree of the N@CFs was responsible for the enhanced activity in selective  $\text{H}_2\text{S}$  oxidation.<sup>108</sup> This conclusion was much different that that reached by Long *et al.*, who illustrated that the pyridinic nitrogen species are responsible for the catalytic activity for  $\text{H}_2\text{S}$  oxidation in the presence of nitrogen-doped mesoporous carbons (NMC).<sup>119</sup> Encouraged by the promoting effect of nitrogen doping, NPC materials have been also used as metal-free catalysts in the oxidation  $\text{NO}$  to  $\text{NO}_2$  with enhanced activities,<sup>75,82,120</sup> and it seems that both pyridinic and pyrrolic nitrogen species are favorable for  $\text{NO}$  oxidation.<sup>120</sup> Therefore, depending on the preparation method and physicochemical properties of the various NPC materials, the conclusions on the active sites responsible for improving the oxidation activity may differ.

An early example of the metal-free oxidation of benzyl alcohol using NPC materials was reported by the Wang group, who found that nitrogen-doped graphene (NG) demonstrated greatly enhanced activity compared to non-doped graphene.<sup>97</sup> Through a detailed surface analysis of a series of NGs prepared at different temperatures, the authors revealed the structure-performance relationship of NG and demonstrated that the metal-free catalysis takes place at graphitic  $\text{sp}^2$  nitrogen sites. Notably, the authors suggested that the high selectivities for primary aldehydes (up to 100%) were due to a catalytic oxidation mechanism that is more likely without deep oxidation frequently induced by the produced byproduct  $\text{H}_2\text{O}_2$ . The use of an EPR spin-trapping technique and a photometric method verified this idea because no other active oxygen species (*e.g.*,  $\text{O}_2^{\cdot-}$ ,  $\cdot\text{OH}$ , or  $\text{H}_2\text{O}_2$ ) were observed in the reaction process. Therefore, an  $\text{sp}^2$  N– $\text{O}_2$  adduct transition state was proposed to be involved in the following reaction mechanism: the adsorption and activation of molecular oxygen over the graphitic N active sites form a highly chemical reactive  $\text{sp}^2$  N– $\text{O}_2$  adduct transition state, which in turn directly attacks the  $\alpha$ -H atom of the alcohol to form water (Scheme 6). A similar observation that the activity originates from the graphitic nitrogen species was also reported by



**Scheme 6** Proposed reaction pathway for aerobic alcohol oxidation over N-doped graphene nanosheets. Reproduced with permission from ref. 97. Copyright© 2012 American Chemical Society.

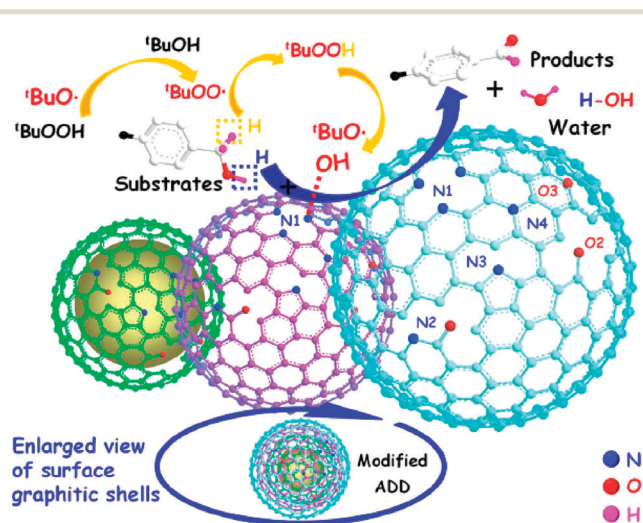
Masahiko Arai and coworkers. The authors gave some clues regarding the stability of this active center: the graphitic nitrogen species are likely to change to the less active oxidized ones, causing catalyst deactivation during the oxidation reaction; this deactivation could not be avoided due to the nature of the reaction.<sup>55</sup> However, conclusions on the monotonic correlations with specific nitrogen species may not be easily drawn due to the structural and morphological complexity of the used NPC materials (e.g., NCNTs).<sup>185</sup> Furthermore, a reaction mechanism involving radicals was often observed in the NPC-catalyzed metal-free oxidation of benzyl alcohols,<sup>33,55,184</sup> which is a different from the non-radical process illustrated by Wang *et al.*<sup>97</sup>

Notably, the Su group did a good job of employing NPC materials as metal-free catalysts for benzyl alcohol oxidation, demonstrating that pyridinic nitrogen species are the active sites for the catalytic oxidation of benzyl alcohol. The formation and transformation pathways of nitrogen species and a reaction mechanism involving free radicals were elaborated in detail.<sup>33</sup> An interesting hybrid material, annealed ultradispersed nanodiamond (ADD), with  $sp^2$  curved concentric graphitic shells combining the remarkable surface properties of graphene-based nanomaterials with the intrinsic properties of a diamond core was selected as the starting material for nitrogen-modified ADD (N-ADD) powder *via* three different preparation methods in a calcinations treatment process. XPS analyses of the resulting N-ADD samples and the pristine ADD powder revealed a significant increase in nitrogen species, particularly pyridinic nitrogen, lactam or cyano nitrogen, and pyrrolic nitrogen species along with a decrease in the atomic ratios of the carbonyl group, carbon-oxygen ether-like single bond and oxygen in pyridine-*N*-oxide and surface trace OH species in the N-ADD samples compared to in ADD. These results suggest that the nitrogen sources may react with some oxygen species in a series of chemical reactions to produce nitrogen species during the preparation process. Through elemental analysis, XPS and temperature-programmed desorption, the authors revealed the detailed formation and dynamic behaviors of the nitrogen species on the modified ADD during the preparation process; the lactam and cyano species function as the intermediates in the formation of various nitrogen species, while the transformation of lactam and cyano species as well as the decomposition and rearrangement of pyridinic or pyrrolic N species contribute to the formation of HCN. By correlating XPS data with the catalytic oxidation of benzylic alcohols in the presence of TBHP, pyridinic N species were found to be the active sites. The following possible reaction pathway was proposed based on the bonding behavior between the pyridinic N species: pyridinic N as a hydrogen bond acceptor reacts with the  $\cdot\text{OH}$  free radical derived from the decomposition of  $\text{tBuOOH}$ , forming pyridinic N-OH active species. These active species capture hydrogen atoms from the alcoholic hydroxyl groups of  $-\text{CH}_2\text{OH}$ , giving rise to the release of water and the formation of  $-\text{CH}_2\text{O}$  groups. The intermediate free radical  $\text{tBuOO}\cdot$  that originated from the reaction of the

decomposer  $\text{tBuO}\cdot$  with a portion of  $\text{tBuOOH}$  can activate the CH bond of the  $-\text{CH}_2\text{O}$  group, finally leading to the formation of a  $-\text{CHO}$  group and  $\text{tBuOOH}$  under mild conditions (Scheme 7).

The activation of hydrocarbon is quite significant due to its vital role in converting basic petrochemical materials into useful compounds. However, this task remains a great challenge in both academia and industry because of the high dissociation energy of the C-H bond.<sup>192</sup> Current approaches for efficient C-H bond activation are mostly based on the employment of transition metals or organometallic centers.<sup>193</sup> Outside of the use of metals, NPC materials as metal-free catalysts have also demonstrated their use in the activation of various kinds of C-H bonds, even under moderate reaction conditions.<sup>32,81,124,136,186</sup>

The activity of NPC materials was initially predicated through theoretical calculations by Hu and coworkers, who illustrated that the catalytic ability of metal-free NCNT is comparable to those reported for noble metal catalysts and enzymes for methane C-H activation through the activated adsorbed oxygen atoms.<sup>194</sup> Almost at the same time, experimental studies by the Peng group demonstrated the high activities of NCNTs in the activation of the C-H bond through the aerobic oxidation of cyclohexane in the liquid phase.<sup>124</sup> The authors found that the reaction proceeds through a radical-involved autoxidation process, and the activity was enhanced in the presence of cyclohexanone, which catalyzes the initiation of a chain reaction. Interestingly, compared with undoped CNTs, the NCNTs generated over two-times greater reaction rates. This enhancement was attributed to the enhanced electron transfer in the NCNTs, as evidenced by the more stable radical-NCNT complex compared to the radical-CNT complex calculated by DFT. Furthermore, the conversion of  $\text{C}_6\text{H}_{12}$  increased with annealing temperature, indicating



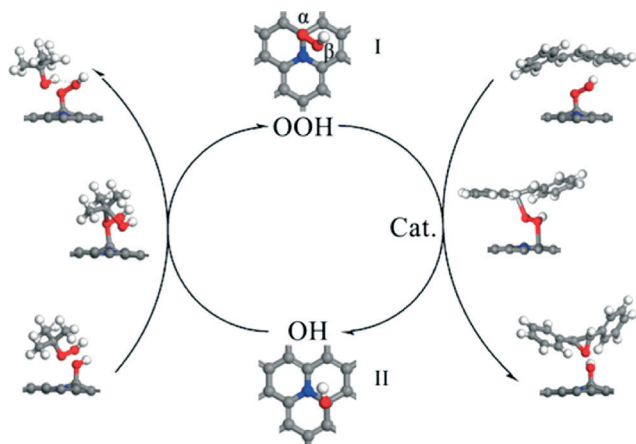
Scheme 7 Mechanism diagram of catalytic reaction for benzylic alcohols on modified ADD (three graphitic shells are used as an ideal catalyst model). Reproduced with permission from ref. 33. Copyright© 2014 American Chemical Society.

that CNTs with higher long-range order and electron delocalization are preferred. This observation further demonstrated that the introduction of electron-donating nitrogen species in the graphitic domains can further improve the activity as a result of enhanced electron transfer. These types of NCNTs were further applied to other kinds of C–H bonds, including the selective oxidation of cumene to acetophenone and 2-benzyl-2-propanol<sup>122</sup> and the selective allylic oxidation of cyclohexene to 2-cyclohexen-1-one.<sup>104</sup>

This great potential of NCNTs in the activation of C–H bonds has inspired researchers to develop novel NPC materials towards this end. Indeed, another inspiring work was reported by the Ma group, who demonstrated the fantastic catalytic performance of a nitrogen-doped  $sp^2$ -hybridized graphene in liquid-phase C–H bond oxidation.<sup>32</sup> Initially, the authors employed Arc-C (a graphene sample prepared by the arc-discharge method) and LC (a layered carbon prepared by the pyrolytic method with graphene oxide as the precursor) with different BET specific areas ( $61.3 \text{ m}^2 \text{ g}^{-1}$  for Arc-C and  $423.6 \text{ m}^2 \text{ g}^{-1}$  for LC) as the catalysts for the liquid-phase oxidation of ethylbenzene in the presence of TBHP; however, the two catalysts both gave moderate but similar acetophenone yields (20.7% and 27.3%, respectively). This strange result suggests that the catalytic activity is not directly related to the surface area of the catalyst, and the authors proposed that the trace nitrogen content in the carbons may be the key factor. Therefore, the relationship between the nitrogen content of the catalyst and its catalytic activity was investigated. The authors concluded that nitrogen doping indeed promotes the high activity in C–H activation; particularly, the graphitic nitrogen species may be the most influential.<sup>32</sup> However, whether the nitrogen itself participates in activating reactants remains unclear. Therefore, detailed investigations using X-ray absorption spectroscopy (XAS) and DFT calculations were performed. The results suggested that the graphitic-type nitrogen dopant does not directly participate in the activation of the C–H bonds of the reactant, and the excellent performance of the LC–N catalysts is due to the ability of carbon to host the reactive oxygen species with the introduction of nitrogen. This was further verified by studying the electronic partial density of states (PDOS) along with the charges of nitrogen and carbon in different positions (*ortho*-, *meta*-, and *para*-carbon atoms and carbon atoms far away from the doped nitrogen (referred to as f-carbon)). The much stronger DOS intensities near the Fermi level for *ortho*-carbon confers the *ortho*-carbon a metal-like d-band electronic structure, thus contributing to a metal-like catalytic performance. The much larger compensating positive charge modified by the nitrogen dopant also makes *ortho*-carbon a superior position for the adsorption of reactive oxygen species such as peroxide. This work provided a detailed investigation of the origin of the activity resulting from the incorporation of nitrogen dopants in the carbon structure; the results suggested that nitrogen atoms at graphitic-type sites in layered carbon catalysts are pivotal for C–H bond activation. The nitrogen dopant did not participate in the activation of

reactant; instead, the peroxide groups generated on the surface of the catalyst are the active oxygen species on the surface of the nitrogen-doped layered carbon catalyst.

Encouraged by the attractive properties of NCNTs and N-graphene in C–H bond activation, more sustainable syntheses of these types of materials are welcome. For example, biomass-derived chitosan was used as a precursor for the fabrication of nitrogen-doped graphene, which serves as an active metal-free catalyst for the activation of a series of C–H bonds, including cyclooctane, diphenylmethane, indane, and ethylbenzene.<sup>186</sup> An eco-efficient simultaneous microsonochemical reduction (MR) process was used to prepare N-graphene in 70 min by introducing aqueous solutions of GO and hydrazine hydrate into a capillary microreactor, producing aromatic and aliphatic ketone products *via* the activation of a series of C–H bonds.<sup>81</sup> In addition, other types of NPC materials are stepping into this area, although they remain at the early stage. For example, an N-doped ordered mesoporous carbon (NOMC) was successfully fabricated and applied in the activation of ethylbenzene.<sup>136</sup> However, because of the high dissociation energy of the C–H bond, only limited metal-free carbon materials have been shown to be active in the liquid-phase oxidation of C–H. Thus, it is highly desirable to develop novel metal-free carbon materials, mainly those with nitrogen decoration, using sustainable fabrication techniques in order to achieve highly reactive materials to activate more stable substrates such as methylbenzene. Another less studied oxidation reaction in the NPC-based metal-free system is the selective epoxidation of alkenes to their corresponding epoxides, which are important intermediates for the syntheses of perfume, drugs, epoxy resins, sweeteners, *etc.* The Ma group tested N-doped graphene as a highly reactive catalyst in the epoxidation of *trans*-stilbene; they obtained 95.8% conversion and 94.4% selectivity for *trans*-stilbene epoxide.<sup>56</sup> Based on the ability of nitrogen doing to increase both catalytic activity and *trans*-stilbene epoxide selectivity, the authors conducted experiments to explore the origins of these effects. By changing the nitrogen doping *via* GO treatment in  $\text{NH}_3$  atmosphere under temperatures ranging from 200–800 °C, a series of NG materials with nitrogen contents ranging from 0.42–1.29 at% were obtained. The reactivity was not correlated with the nitrogen content. However, interestingly, the authors observed a linear relationship between the graphitic nitrogen concentration and the epoxidation activity, which was consistent with their earlier conclusion.<sup>32</sup> After eliminating the contributions of residual Fe and the synergic effect of Fe and nitrogen, the authors concluded that the activity originated only from the graphitic nitrogen species; the graphitic nitrogen dopant did not participate in the epoxidation reaction, but rather modulated the electronic structure of the  $sp^2$  carbon material.<sup>32</sup> Thus, the authors carried out DFT calculations to illustrate the oxidation mechanism of the carbon–carbon double bonds (Scheme 8). Although the formation of reactive oxygen species was governed by the modulated electronic structure of the N-doped graphene catalysts, the unique



**Scheme 8** The reaction mechanism for the epoxidation of *trans*-stilbene on a nitrogen-doped graphene catalyst. Reproduced with permission from ref. 56. Copyright© 2014 American Chemical Society.

geometric feature described is responsible for the epoxidation, specifically the transferring/hopping of hydroxyls and the successive recycling of the reactive oxygen species. This NG catalyst could be recycled more than five times without losing activity and selectivity; it was also highly active and selective in the epoxidation of styrene (with 87.6% conversion and 72.8% epoxide selectivity).<sup>56</sup> Similar to the observations of the Ma group, Su and coworkers applied another kind of NPC N-doped onion-like carbon in the epoxidation of styrene; although this material showed inferior selectivity (46%), this work further elucidated the role of graphitic nitrogen in promoting epoxidation and epoxide selectivity.<sup>76</sup>

## 5. Conclusions and outlook

The highly porous microstructure (mainly mesoporous structure) and beneficial nitrogen functionalities of NPC materials combined with a deep knowledge of their active sites through novel characterizations to theoretical modeling have enabled the wide use of NPC materials as catalysts or catalyst supports. In this review, we introduced the various fabrication techniques for nitrogen-doped porous carbon materials and discussed their many applications in heterogeneous hydrogenations and oxidations. The specific interaction of the incorporated nitrogen heteroatom with supported metals (both noble and non-noble metals), which contributes to good dispersion, smaller particle size, and modified electronic states of supported metal NPs, makes NPC materials promising catalyst supports in both hydrogenations and oxidations.<sup>27,31,43,95</sup> Further, the modified charge distributions of NPC materials also induces novel active sites and activation modes, further enabling NPC materials as metal-free catalyst with enhanced catalytic oxidation activities towards alcohols and hydrocarbons.<sup>32,33,124</sup>

Although the applications of NPC materials in heterogeneous hydrogenations and oxidations have seen great advancements, a deeper understanding of the origins of their

activity still remains to be investigated. When serving as supports, the investigation of the correlation between structure and properties will continue to be a key topic of future studies. Specifically, how the interaction between the supported metal and nitrogen influences reaction activity remains an interesting area of study. The solutions are expected to be found using experimental trials combined with theoretical calculations, which will help us better understand the reaction mechanism and the active sites (nitrogen doping), which in turn may provide theoretical guidance for designing and preparing highly active and selective catalysts. The great achievements of NPC materials in metal-free catalysis could deepen our understanding of their properties and detailed reaction mechanisms. However, with respect to industrial manufacturing, it seems more promising to combine the advantages of metal NPs.

Therefore, future studies are expected to further modify supported catalysts in two ways, by modifying metal NPs and the NPC supports. As for metal NPs, studies on developing bi/multi-metal-based alloys hybridized with NPC materials should be intensified due to the possibility of enhanced catalytic performance resulting from the synergic effects among the different components in hybrid catalysts.<sup>25,26</sup> When it comes to the design of catalyst supports, it is highly suggested to develop supports with 3D pore structure for their advantage in contributing to the mass transfer in reactions. Therefore, the one-step and low-cost production in large quantities will be increasingly appreciated. Notably, these directions are still new in the area of NPC-based supported catalysts; however, they show promising prospects, and it is hoped that more breakthroughs will be achieved in these respects.

There are still many challenges related to practical hydrogenations and oxidations. In hydrogenations, the key challenge is to selectively hydrogenate targeted functional groups in the presence of multiple reduction groups. There is a bright future in developing highly active and selective hydrogenation catalysts for the synthesis of fine chemicals and for the refining of biomass to manufacture bio-oils. As for the more complex oxidation reactions, which easily produce byproducts, developing active catalysts while maintaining the product selectivity will continue to be a great challenge. Notably, supported NPC catalysts are expected to play significant roles in activating a series of substrates that are difficult to activate, such as cyclohexane, benzene, toluene and methane.

This review covers the state-of-art fabrication of various NPC materials and their bright future as promising catalysts or catalyst supports for heterogeneous hydrogenations and oxidations. And the correlations between their excellent catalytic performance and the unique features of NPC materials were also elucidated. Less discussed in this review are the various advanced characterization techniques combined with theoretical modeling, which are highly important in designing NPC materials in rational ways and in understanding the tested reactions in detail. The reader is referred to the excellent review by Su *et al.* for a detailed discussion of these methods.<sup>18</sup>

## Acknowledgements

Financial support from the National Natural Science Foundation of China (91534114 & 21376208), the Zhejiang Provincial Natural Science Foundation for Distinguished Young Scholars of China (LR13B030001), the Fundamental Research Funds for the Central Universities, the Program for Zhejiang Leading Team of S&T Innovation, the Partner Group Program of the Zhejiang University and the Max-Planck Society is greatly appreciated.

## References

- J. Hagen, *Industrial Catalysis: A Practical Approach*, Wiley-VCH Verlag GmbH & Co. KGaA, 2nd edn, 2006.
- J. A. Dumesic, G. W. Huber, and M. Boudart, *Handbook of Heterogeneous catalysis*, Wiley-VCH Verlag GmbH & Co. KGaA, 2008.
- T. F. S. Silva, G. S. Mishra, M. F. Guedes da Silva, R. Wanke, L. M. D. R. S. Martins and A. J. L. Pombeiro, *Dalton Trans.*, 2009, 9207–9215, DOI: 10.1039/B911990F.
- H. Liu, T. Jiang, B. Han, S. Liang and Y. Zhou, *Science*, 2009, **326**, 1250–1252.
- T. Hayashi, K. Tanaka and M. Haruta, *J. Catal.*, 1998, **178**, 566–575.
- E. J. Corey and G. Schmidt, *Tetrahedron Lett.*, 1979, 399–402.
- J. W. Ladbury and C. F. Cullis, *Chem. Rev.*, 1958, **58**, 403–438.
- J. Muzart, *Chem. Rev.*, 1992, **92**, 113–140.
- U. Schuchardt, D. Cardoso, R. Sercheli, R. Pereira, R. S. da Cruz, M. C. Guerreiro, D. Mandelli, E. V. Spinacé and E. L. Pires, *Appl. Catal., A*, 2001, **211**, 1–17.
- Y. Wang, J. Zhang, X. Wang, M. Antonietti and H. Li, *Angew. Chem., Int. Ed.*, 2010, **49**, 3356–3359.
- S. G. Shore, E. Ding, C. Park and M. A. Keane, *J. Mol. Catal. A: Chem.*, 2004, **212**, 291–300.
- M. Chatterjee, H. Kawanami, M. Sato, A. Chatterjee, T. Yokoyama and T. Suzuki, *Adv. Synth. Catal.*, 2009, **351**, 1912–1924.
- Y. Wang, J. Yao, H. Li, D. Su and M. Antonietti, *J. Am. Chem. Soc.*, 2011, **133**, 2362–2365.
- A. Cybulski, J. A. Moulijn, M. M. Sharma and R. A. Sheldon, *Fine Chemicals Manufacture-Technology and Engineering*, Elsevier, Amsterdam, 2001.
- D. Astruc, F. Lu and J. R. Aranzas, *Angew. Chem., Int. Ed.*, 2005, **44**, 7852–7872.
- S. Mandal, D. Roy, R. V. Chaudhari and M. Sastry, *Chem. Mater.*, 2004, **16**, 3714–3724.
- A. Dhakshinamoorthy and H. Garcia, *Chem. Soc. Rev.*, 2012, **41**, 5262–5284.
- D. S. Su, S. Perathoner and G. Centi, *Chem. Rev.*, 2013, **113**, 5782–5816.
- T. Mallat and A. Baiker, *Chem. Rev.*, 2004, **104**, 3037–3058.
- Y. Wang, X. Wang and M. Antonietti, *Angew. Chem., Int. Ed.*, 2012, **51**, 68–89.
- Z. A. Qiao, P. Zhang, S. H. Chai, M. Chi, G. M. Veith, N. C. Gallego, M. Kidder and S. Dai, *J. Am. Chem. Soc.*, 2014, **136**, 11260–11263.
- L. Kesavan, R. Tiruvalam, M. H. Ab Rahim, M. I. bin Saiman, D. I. Enache, R. L. Jenkins, N. Dimitratos, J. A. Lopez-Sanchez, S. H. Taylor, D. W. Knight, C. J. Kiely and G. J. Hutchings, *Science*, 2011, **331**, 195–199.
- A. S. K. Hashmi and G. J. Hutchings, *Angew. Chem., Int. Ed.*, 2006, **45**, 7896–7936.
- Z. Li, J. Liu, C. Xia and F. Li, *ACS Catal.*, 2013, **3**, 2440–2448.
- P. Zhang, J. Yuan, T.-P. Fellingner, M. Antonietti, H. Li and Y. Wang, *Angew. Chem., Int. Ed.*, 2013, **52**, 6028–6032.
- M. Tang, S. Mao, M. Li, Z. Wei, F. Xu, H. Li and Y. Wang, *ACS Catal.*, 2015, 3100–3107.
- R. V. Jagadeesh, A.-E. Surkus, H. Junge, M.-M. Pohl, J. Radnik, J. Rabeah, H. Huan, V. Schünemann, A. Brückner and M. Beller, *Science*, 2013, **342**, 1073–1076.
- R. V. Jagadeesh, T. Stemmler, A.-E. Surkus, M. Bauer, M.-M. Pohl, J. Radnik, K. Junge, H. Junge, A. Brückner and M. Beller, *Nat. Protoc.*, 2015, **10**, 916–926.
- R. V. Jagadeesh, T. Stemmler, A.-E. Surkus, H. Junge, K. Junge and M. Beller, *Nat. Protoc.*, 2015, **10**, 548–557.
- Z. Wei, J. Wang, S. Mao, D. Su, H. Jin, Y. Wang, F. Xu, H. Li and Y. Wang, *ACS Catal.*, 2015, **5**, 4783–4789.
- P. Zhang, Y. Gong, H. Li, Z. Chen and Y. Wang, *Nat. Commun.*, 2013, **4**, 1593.
- Y. Gao, G. Hu, J. Zhong, Z. Shi, Y. Zhu, D. S. Su, J. Wang, X. Bao and D. Ma, *Angew. Chem., Int. Ed.*, 2013, **52**, 2109–2113.
- Y. Lin and D. Su, *ACS Nano*, 2014, **8**, 7823–7833.
- R. C. Bansal, J. B. Donnet and F. Stoeckli, *Active Carbon*, Marcel Dekker, New York, 1988.
- T. R. Gaffney, *Curr. Opin. Solid State Mater. Sci.*, 1996, **1**, 69.
- W. M. A. W. Daud and A. H. Houshamnd, *J. Nat. Gas Chem.*, 2010, **19**, 267.
- V. Calvino-Casilda, A. J. López-Peinado, C. J. Duran-Valle and R. M. Martin-Aranda, *Catal. Rev.: Sci. Eng.*, 2010, **52**, 325.
- J. C. S. Wu, Z. A. Lin, F. M. Tsai and J. W. Pan, *Catal. Today*, 2000, **63**, 419–426.
- A. Savara, C. E. Chan-Thaw, I. Rossetti, A. Villa and L. Prati, *ChemCatChem*, 2014, 3464–3473.
- Z. Li, J. Li, J. Liu, Z. Zhao, C. Xia and F. Li, *ChemCatChem*, 2014, **6**, 1333–1339.
- K. Gong, F. Du, Z. Xia, M. Durstock and L. Dai, *Science*, 2009, **323**, 760–764.
- L.-F. Chen, X.-D. Zhang, H.-W. Liang, M. Kong, Q.-F. Guan, P. Chen, Z.-Y. Wu and S.-H. Yu, *ACS Nano*, 2012, **6**, 7092–7102.
- X. Xu, Y. Li, Y. Gong, P. Zhang, H. Li and Y. Wang, *J. Am. Chem. Soc.*, 2012, **134**, 16987–16990.
- J. H. Knox, B. Kaur and G. R. Millward, *J. Chromatogr.*, 1986, **352**, 3–25.
- R. Ryoo, S. H. Joo and S. Jun, *J. Phys. Chem. B*, 1999, **103**, 7743–7746.
- N. Fechner, T.-P. Fellingner and M. Antonietti, *Adv. Mater.*, 2013, **25**, 75–79.

- 47 X. Liu and M. Antonietti, *Adv. Mater.*, 2013, 25, 6284–6290.
- 48 J. Deng, T. Xiong, F. Xu, M. Li, C. Han, Y. Gong, H. Wang and Y. Wang, *Green Chem.*, 2015, 17, 4053–4060.
- 49 C. Liang, K. Hong, G. A. Guiochon, J. W. Mays and S. Dai, *Angew. Chem., Int. Ed.*, 2004, 43, 5785–5789.
- 50 S. Tanaka, N. Nishiyama, Y. Egashira and K. Ueyama, *Chem. Commun.*, 2005, 2125–2127.
- 51 Y. Meng, D. Gu, F. Zhang, Y. Shi, H. Yang, Z. Li, C. Yu, B. Tu and D. Zhao, *Angew. Chem., Int. Ed.*, 2005, 44, 7053–7059.
- 52 V. Budarin, J. H. Clark, J. J. Hardy, R. Luque, K. Milkowski, S. J. Tavener and A. J. Wilson, *Angew. Chem., Int. Ed.*, 2006, 45, 3782–3786.
- 53 R. Nie, M. Miao, W. Du, J. Shi, Y. Liu and Z. Hou, *Appl. Catal., B*, 2016, 180, 607–613.
- 54 M. N. Groves, A. S. W. Chan, C. Malardier-Jugroot and M. Jugroot, *Chem. Phys. Lett.*, 2009, 481, 214–219.
- 55 H. Watanabe, S. Asano, S.-I. Fujita, H. Yoshida and M. Arai, *ACS Catal.*, 2015, 5, 2886–2894.
- 56 W. Li, Y. Gao, W. Chen, P. Tang, W. Li, Z. Shi, D. Su, J. Wang and D. Ma, *ACS Catal.*, 2014, 4, 1261–1266.
- 57 P. Ayala, R. Arenal, M. Ruemmeli, A. Rubio and T. Pichler, *Carbon*, 2010, 48, 575–586.
- 58 H. Wang, T. Maiyalagan and X. Wang, *ACS Catal.*, 2012, 2, 781–794.
- 59 W. Shen and W. Fan, *J. Mater. Chem. A*, 2013, 1, 999–1013.
- 60 K. N. Wood, R. O'Hayre and S. Pylypenko, *Energy Environ. Sci.*, 2014, 7, 1212.
- 61 O. Y. Podyacheva and Z. R. Ismagilov, *Catal. Today*, 2015, 249, 12–22.
- 62 X.-H. Li and M. Antonietti, *Chem. Soc. Rev.*, 2013, 42, 6593–6604.
- 63 P. Ayala, R. Arenal, M. Rummeli, A. Rubio and T. Pichler, *Carbon*, 2010, 48, 575–586.
- 64 X. K. Kong, C. L. Chen and Q. W. Chen, *Chem. Soc. Rev.*, 2014, 43, 2841–2857.
- 65 M. Li, X. Xu, Y. Gong, Z. Wei, Z. Hou, H. Li and Y. Wang, *Green Chem.*, 2014, 16, 4371–4377.
- 66 M. Tang, S. Mao, M. Li, Z. Wei, F. Xu, H. Li and Y. Wang, *ACS Catal.*, 2015, 5, 3100–3107.
- 67 F. A. Westerhaus, R. V. Jagadeesh, G. Wienhöfer, M.-M. Pohl, J. Radnik, A.-E. Surkus, J. Rabeah, K. Junge, H. Junge, M. Nielsen, A. Brückner and M. Beller, *Nat. Chem.*, 2013, 5, 537–543.
- 68 J. Lee, J. Kim and T. Hyeon, *Adv. Mater.*, 2006, 18, 2073–2094.
- 69 R. J. White, V. Budarin, R. Luque, J. H. Clark and D. J. Macquarrie, *Chem. Soc. Rev.*, 2009, 38, 3401.
- 70 Y. Xia, Z. Yang and R. Mokaya, *Nanoscale*, 2010, 2, 639–659.
- 71 M.-M. Titirici, R. J. White, N. Brun, V. L. Budarin, D. S. Su, F. del Monte, J. H. Clark and M. J. MacLachlan, *Chem. Soc. Rev.*, 2015, 44, 250–290.
- 72 L. Chuenchom, R. Kraehnert and B. M. Smarsly, *Soft Matter*, 2012, 8, 10801.
- 73 C. Liang, Z. Li and S. Dai, *Angew. Chem., Int. Ed.*, 2008, 47, 3696–3717.
- 74 P. Zhang, H. Zhu and S. Dai, *ChemCatChem*, 2015, 7, 2788–2805.
- 75 M.-X. Wang, Z. Guo, Z.-H. Huang and F. Kang, *Catal. Commun.*, 2015, 62, 83–88.
- 76 Y. Lin, X. Pan, W. Qi, B. Zhang and D. S. Su, *J. Mater. Chem. A*, 2014, 2, 12475–12483.
- 77 S.-i. Fujita, H. Watanabe, A. Katagiri, H. Yoshida and M. Arai, *J. Mol. Catal. A: Chem.*, 2014, 393, 257–262.
- 78 S. Abate, R. Arrigo, M. E. Schuster, S. Perathoner, G. Centi, A. Villa, D. Su and R. Schlögl, *Catal. Today*, 2010, 157, 280–285.
- 79 P. Liu, G. Li, W.-T. Chang, M.-Y. Wu, Y.-X. Li and J. Wang, *RSC Adv.*, 2015, 5, 72785–72792.
- 80 S. Chen, P. Qi, J. Chen and Y. Yuan, *RSC Adv.*, 2015, 5, 31566–31574.
- 81 A. K. Singh, K. C. Basavaraju, S. Sharma, S. Jang, C. P. Park and D.-P. Kim, *Green Chem.*, 2014, 16, 3024–3030.
- 82 J. P. S. Sousa, M. F. R. Pereira and J. L. Figueiredo, *Catal. Today*, 2011, 176, 383–387.
- 83 E. Raymundo-Piñero, D. Cazorla-Amorós and A. Linares-Solano, *Carbon*, 2003, 41, 1925–1932.
- 84 S. Indrawirawan, H. Sun, X. Duan and S. Wang, *J. Mater. Chem. A*, 2015, 3, 3432–3440.
- 85 X. Duan, K. O'Donnell, H. Sun, Y. Wang and S. Wang, *Small*, 2015, 11, 3036–3044.
- 86 H. Sun, Y. Wang, S. Liu, L. Ge, L. Wang, Z. Zhu and S. Wang, *Chem. Commun.*, 2013, 49, 9914–9916.
- 87 Z. Zhao, Y. Dai, G. Ge and G. Wang, *ChemCatChem*, 2015, 7, 1135–1144.
- 88 Z. Zhao, Y. Dai, G. Ge and G. Wang, *Chem. – Eur. J.*, 2015, 21, 8004–8009.
- 89 Z. Zhao, Y. Dai, G. Ge, X. Guo and G. Wang, *RSC Adv.*, 2015, 5, 53095–53099.
- 90 Z. Zhao, Y. Dai, G. Ge, X. Guo and G. Wang, *Green Chem.*, 2015, 17, 3723–3727.
- 91 Z. Zhao, Y. Dai, G. Ge, X. Guo and G. Wang, *Phys. Chem. Chem. Phys.*, 2015, 17, 18895–18899.
- 92 M. Zhang, J. Shi, Y. Sun, W. Ning and Z. Hou, *Catal. Commun.*, 2015, 70, 72–76.
- 93 R. Nie, J. Shi, W. Du, W. Ning, Z. Hou and F.-S. Xiao, *J. Mater. Chem. A*, 2013, 1, 9037–9045.
- 94 R. V. Jagadeesh, H. Junge, M.-M. Pohl, J. Radnik, A. Brueckner and M. Beller, *J. Am. Chem. Soc.*, 2013, 135, 10776–10782.
- 95 F. A. Westerhaus, R. V. Jagadeesh, G. Wienhoefer, M.-M. Pohl, J. Radnik, A.-E. Surkus, J. Rabeah, K. Junge, H. Junge, M. Nielsen, A. Brueckner and M. Beller, *Nat. Chem.*, 2013, 5, 537–543.
- 96 B. Stöhr, H. P. Boehm and R. Schlögl, *Carbon*, 1991, 29, 707–720.
- 97 J. Long, X. Xie, J. Xu, Q. Gu, L. Chen and X. Wang, *ACS Catal.*, 2012, 2, 622–631.
- 98 R. V. Jagadeesh, K. Natte, H. Junge and M. Beller, *ACS Catal.*, 2015, 5, 1526–1529.
- 99 A. V. Iosub and S. S. Stahl, *Org. Lett.*, 2015, 17, 4404–4407.

- 100 X. Cui, Y. Li, S. Bachmann, M. Scalone, A.-E. Surkus, K. Junge, C. Topf and M. Beller, *J. Am. Chem. Soc.*, 2015, **137**, 10652–10658.
- 101 D. Banerjee, R. V. Jagadeesh, K. Junge, M. M. Pohl, J. Radnik, A. Bruckner and M. Beller, *Angew. Chem., Int. Ed.*, 2014, **53**, 4359–4363.
- 102 F. Chen, A.-E. Surkus, L. He, M.-M. Pohl, J. Radnik, C. Topf, K. Junge and M. Beller, *J. Am. Chem. Soc.*, 2015, **137**, 11718–11724.
- 103 R. V. Jagadeesh, H. Junge and M. Beller, *Nat. Commun.*, 2014, **5**, 4123.
- 104 Y. Cao, H. Yu, F. Peng and H. Wang, *ACS Catal.*, 2014, **4**, 1617–1625.
- 105 R. Palkovits, M. Antonietti, P. Kuhn, A. Thomas and F. Schüth, *Angew. Chem., Int. Ed.*, 2009, **48**, 6909–6912.
- 106 W. Zhong, H. Liu, C. Bai, S. Liao and Y. Li, *ACS Catal.*, 2015, **5**, 1850–1856.
- 107 K. Shen, L. Chen, J. Long, W. Zhong and Y. Li, *ACS Catal.*, 2015, **5**, 5264–5271.
- 108 Y. Liu, C. Duong-Viet, J. Luo, A. Hébraud, G. Schlatter, O. Ersen, J.-M. Nhut and C. Pham-Huu, *ChemCatChem*, 2015, **7**, 2957–2964.
- 109 Y. Bide, M. R. Nabid and F. Dastar, *RSC Adv.*, 2015, **5**, 63421–63428.
- 110 X. Xu, H. Li and Y. Wang, *ChemCatChem*, 2014, **6**, 3328–3332.
- 111 R. Liu, S. M. Mahurin, C. Li, R. R. Unocic, J. C. Idrobo, H. Gao, S. J. Pennycook and S. Dai, *Angew. Chem., Int. Ed.*, 2011, **50**, 6799–6802.
- 112 J. Wang, Z. Wei, Y. Gong, S. Wang, D. Su, C. Han, H. Li and Y. Wang, *Chem. Commun.*, 2015, **51**, 12859–12862.
- 113 J. Wang, H. Liu, J. Diao, X. Gu, H. Wang, J. Rong, B. Zong and D. S. Su, *J. Mater. Chem. A*, 2015, **3**, 2305–2313.
- 114 R. P. Rocha, J. Restivo, J. P. S. Sousa, J. J. M. Órfão, M. F. R. Pereira and J. L. Figueiredo, *Catal. Today*, 2015, **241**, 73–79.
- 115 Y. Hao, S. Wang, Q. Sun, L. Shi and A.-H. Lu, *Chin. J. Catal.*, 2015, **36**, 612–619.
- 116 O. A. Stonkus, L. S. Kibis, O. Yu. Podyacheva, E. M. Slavinskaya, V. I. Zaikovskii, A. H. Hassan, S. Hampel, A. Leonhardt, Z. R. Ismagilov, A. S. Noskov and A. I. Boronin, *ChemCatChem*, 2014, **6**, 2115–2128.
- 117 O. Y. Podyacheva, A. I. Stadnichenko, S. A. Yashnik, O. A. Stonkus, E. M. Slavinskaya, A. I. Boronin, A. V. Puzynin and Z. R. Ismagilov, *Chin. J. Catal.*, 2014, **35**, 960–969.
- 118 A. B. Ayusheev, O. P. Taran, I. A. Seryak, O. Y. Podyacheva, C. Descorme, M. Besson, L. S. Kibis, A. I. Boronin, A. I. Romanenko, Z. R. Ismagilov and V. Parmon, *Appl. Catal., B*, 2014, **146**, 177–185.
- 119 F. Sun, J. Liu, H. Chen, Z. Zhang, W. Qiao, D. Long and L. Ling, *ACS Catal.*, 2013, **3**, 862–870.
- 120 J. P. S. Sousa, M. F. R. Pereira and J. L. Figueiredo, *Appl. Catal., B*, 2012, **125**, 398–408.
- 121 X. Ning, H. Yu, F. Peng and H. Wang, *J. Catal.*, 2015, **325**, 136–144.
- 122 S. Liao, Y. Chi, H. Yu, H. Wang and F. Peng, *ChemCatChem*, 2014, **6**, 555–560.
- 123 C. Chen, J. Zhang, B. Zhang, C. Yu, F. Peng and D. Su, *Chem. Commun.*, 2013, **49**, 8151–8153.
- 124 H. Yu, F. Peng, J. Tan, X. Hu, H. Wang, J. Yang and W. Zheng, *Angew. Chem., Int. Ed.*, 2011, **50**, 3978–3982.
- 125 S.-W. Bian, S. Liu, M.-X. Guo, L.-L. Xu and L. Chang, *RSC Adv.*, 2015, **5**, 11913–11916.
- 126 I. Nongwe, V. Ravat, R. Meijboom and N. J. Coville, *Appl. Catal., A*, 2013, **466**, 1–8.
- 127 M. R. Nabid, Y. Bide and Z. Habibi, *RSC Adv.*, 2015, **5**, 2258–2265.
- 128 X. Xu, M. Tang, M. Li, H. Li and Y. Wang, *ACS Catal.*, 2014, **4**, 3132–3135.
- 129 C. Liu, P. Tang, A. Chen, Y. Hu, Y. Yu, H. Lv and D. Ma, *Mater. Lett.*, 2013, **108**, 285–288.
- 130 A. Chen, Y. Yu, R. Wang, Y. Yu, W. Zang, P. Tang and D. Ma, *Nanoscale*, 2015, **7**, 14684–14690.
- 131 R. Ryoo, S. H. Joo, M. Kruk and M. Jaroniec, *Adv. Mater.*, 2001, **13**, 677–681.
- 132 M. Soorholtz, R. J. White, T. Zimmermann, M.-M. Titirici, M. Antonietti, R. Palkovits and F. Schüth, *Chem. Commun.*, 2013, **49**, 240–242.
- 133 X. Liu and M. Antonietti, *Carbon*, 2014, **69**, 460–466.
- 134 Z. Ma, H. Zhang, Z. Yang, G. Ji, B. Yu, X. Liu and Z. Liu, *Green Chem.*, 2016, **18**, 1976–1982.
- 135 A.-H. Lu, W.-C. Li, W. Schmidt and F. Schüth, *Microporous Mesoporous Mater.*, 2006, **95**, 187–192.
- 136 J. Wang, H. Liu, X. Gu, H. Wang and D. S. Su, *Chem. Commun.*, 2014, **50**, 9182–9184.
- 137 Z. Wei, Y. Gong, T. Xiong, P. Zhang, H. Li and Y. Wang, *Catal. Sci. Technol.*, 2015, **5**, 397–404.
- 138 S. De, A. M. Balu, J. C. van der Waal and R. Luque, *ChemCatChem*, 2015, **7**, 1608–1629.
- 139 J. Ryu, Y.-W. Suh, D. J. Suh and D. J. Ahn, *Carbon*, 2010, **48**, 1990–1998.
- 140 M. Sevilla and A. B. Fuertes, *Carbon*, 2009, **47**, 2281–2289.
- 141 M.-M. Titirici, M. Antonietti and N. Baccile, *Green Chem.*, 2008, **10**, 1204–1212.
- 142 J. Wang, Z. Wei, Y. Gong, S. Wang, D. Su, C. Han, H. Li and Y. Wang, *Chem. Commun.*, 2015, **51**, 12859–12862.
- 143 D. Su, Z. Wei, S. Mao, J. Wang, Y. Li, H. Li, Z. Chen and Y. Wang, *Catal. Sci. Technol.*, 2016, DOI: 10.1039/C5CY02171E.
- 144 A. Nieto-Márquez, D. Toledano, P. Sánchez, A. Romero and J. L. Valverde, *J. Catal.*, 2010, **269**, 242–251.
- 145 V. L. Budarin, J. H. Clark, R. Luque and D. J. Macquarrie, *Chem. Commun.*, 2007, 634–636.
- 146 J. Clark, V. Budarin, T. Dugmore, R. Luque, D. Macquarrie and V. Strelko, *Catal. Commun.*, 2008, **9**, 1709–1714.
- 147 J. Amadou, K. Chizari, M. Houllé, I. Janowska, O. Ersen, D. Bégin and C. Pham-Huu, *Catal. Today*, 2008, **138**, 62–68.
- 148 X. Lepré, E. Terrés, Y. Vega-Cantú, F. J. Rodríguez-Macías, H. Muramatsu, Y. A. Kim, T. Hayashi, M. Endo, M. R. Torres and M. Terrones, *Chem. Phys. Lett.*, 2008, **463**, 124–129.
- 149 N. Ono, *The Nitro Group in Organic Synthesis*, Wiley-VCH, 2001.

- 150 R. S. Downing, P. J. Kunkeler and H. van Bekkum, *Catal. Today*, 1997, **37**, 121–136.
- 151 H.-U. Blaser, H. Steiner and M. Studer, *ChemCatChem*, 2009, **1**, 210–221.
- 152 J. Li, X.-Y. Shi, Y.-Y. Bi, J.-F. Wei and Z.-G. Chen, *ACS Catal.*, 2011, **1**, 657–664.
- 153 A. Corma and P. Serna, *Science*, 2006, **313**, 332–334.
- 154 Y. Gong, M. Li, H. Li and Y. Wang, *Green Chem.*, 2015, **17**, 715–736.
- 155 S. Crossley, J. Faria, M. Shen and D. E. Resasco, *Science*, 2010, **327**, 68–72.
- 156 D. Liu, X. Chen, G. Xu, J. Guan, Q. Cao, B. Dong, Y. Qi, C. Li and X. Mu, *Sci. Rep.*, 2016, **6**, 21365.
- 157 Y.-Z. Chen, G. Cai, Y. Wang, Q. Xu, S.-H. Yu and H.-L. Jiang, *Green Chem.*, 2016, **18**, 1212–1217.
- 158 Z. Zhu, H. Tan, J. Wang, S. Yu and K. Zhou, *Green Chem.*, 2014, **16**, 2636–2643.
- 159 L. Wang, B. Zhang, X. Meng, D. S. Su and F.-S. Xiao, *ChemSusChem*, 2014, **7**, 1537–1541.
- 160 B. S. Moore, H. Cho, R. Casati, E. Kennedy, K. A. Reynolds, U. Mocek, J. M. Beale and H. G. Floss, *J. Am. Chem. Soc.*, 1993, **115**, 5254–5266.
- 161 Z. Tian, Q. Li, Y. Li and S. Ai, *Catal. Commun.*, 2015, **61**, 97–101.
- 162 T. He, L. Liu, G. Wu and P. Chen, *J. Mater. Chem. A*, 2015, **3**, 16235–16241.
- 163 Y. Lee, Y. Motoyama, K. Tsuji, S.-H. Yoon, I. Mochida and H. Nagashima, *ChemCatChem*, 2012, **4**, 778–781.
- 164 Y. Motoyama, Y. Lee, K. Tsuji, S.-H. Yoon, I. Mochida and H. Nagashima, *ChemCatChem*, 2011, **3**, 1578–1581.
- 165 M. Sankar, N. Dimitratos, P. J. Miedziak, P. P. Wells, C. J. Kiely and G. J. Hutchings, *Chem. Soc. Rev.*, 2012, **41**, 8099–8139.
- 166 X. Yang, D. Chen, S. Liao, H. Song, Y. Li, Z. Fu and Y. Su, *J. Catal.*, 2012, **291**, 36–43.
- 167 D. I. Enache, J. K. Edwards, P. Landon, B. Solsona-Espriu, A. F. Carley, A. A. Herzing, M. Watanabe, C. J. Kiely, D. W. Knight and G. J. Hutchings, *Science*, 2006, **311**, 362–365.
- 168 L. Gao, R. Li, X. Sui, R. Li, C. Chen and Q. Chen, *Environ. Sci. Technol.*, 2014, **48**, 10191–10197.
- 169 P. Chen, F. Yang, A. Kostka and W. Xia, *ACS Catal.*, 2014, **4**, 1478–1486.
- 170 X.-K. Kong, Z.-Y. Sun, M. Chen, C.-L. Chen and Q.-W. Chen, *Energy Environ. Sci.*, 2013, **6**, 3260.
- 171 H. Jin, J. Wang, D. Su, Z. Wei, Z. Pang and Y. Wang, *J. Am. Chem. Soc.*, 2015, **137**, 2688–2694.
- 172 O. Y. Podyacheva, Z. R. Ismagilov, A. I. Boronin, L. S. Kibis, E. M. Slavinskaya, A. S. Noskov, N. V. Shikina, V. A. Ushakov and A. V. Ischenko, *Catal. Today*, 2012, **186**, 42–47.
- 173 J. Deng, H. J. Song, M. S. Cui, Y. P. Du and Y. Fu, *ChemSusChem*, 2014, **7**, 3334–3340.
- 174 L. Kesavan, R. Tiruvalam, M. H. Ab Rahim, M. I. bin Saiman, D. I. Enache, R. L. Jenkins, N. Dimitratos, J. A. Lopez-Sanchez, S. H. Taylor, D. W. Knight, C. J. Kiely and G. J. Hutchings, *Science*, 2011, **331**, 195–199.
- 175 A. Villa, D. Wang, P. Spontoni, R. Arrigo, D. Su and L. Prati, *Catal. Today*, 2010, **157**, 89–93.
- 176 X. Xie, J. Long, J. Xu, L. Chen, Y. Wang, Z. Zhang and X. Wang, *RSC Adv.*, 2012, **2**, 12438–12446.
- 177 C. E. Chan-Thaw, A. Villa, L. Prati and A. Thomas, *Chem. – Eur. J.*, 2011, **17**, 1052–1057.
- 178 C. E. Chan-Thaw, A. Villa, P. Katekomol, D. Su, A. Thomas and L. Prati, *Nano Lett.*, 2010, **10**, 537–541.
- 179 D. S. Su, J. Zhang, B. Frank, A. Thomas, X. Wang, J. Paraknowitsch and R. Schlogl, *ChemSusChem*, 2010, **3**, 169–180.
- 180 K. Chizari, A. Deneuve, O. Ersen, I. Florea, Y. Liu, D. Edouard, I. Janowska, D. Begin and C. Pham-Huu, *ChemSusChem*, 2012, **5**, 102–108.
- 181 D.-V. Cuong, L. Truong-Phuoc, T. Tran-Thanh, J.-M. Nhut, L. Nguyen-Dinh, I. Janowska, D. Begin and C. Pham-Huu, *Appl. Catal., A*, 2014, **482**, 397–406.
- 182 X. Duan, H. Sun, Y. Wang, J. Kang and S. Wang, *ACS Catal.*, 2015, **5**, 553–559.
- 183 R. P. Rocha, A. G. Gonçalves, L. M. Pastrana-Martínez, B. C. Bordoni, O. S. G. P. Soares, J. J. M. Órfão, J. L. Faria, J. L. Figueiredo, A. M. T. Silva and M. F. R. Pereira, *Catal. Today*, 2015, **249**, 192–198.
- 184 J. Luo, H. Yu, H. Wang, H. Wang and F. Peng, *Chem. Eng. J.*, 2014, **240**, 434–442.
- 185 J. Luo, F. Peng, H. Wang and H. Yu, *Catal. Commun.*, 2013, **39**, 44–49.
- 186 A. Dhakshinamoorthy, A. Primo, P. Concepcion, M. Alvaro and H. Garcia, *Chem. – Eur. J.*, 2013, **19**, 7547–7554.
- 187 S.-I. Fujita, K. Yamada, A. Katagiri, H. Watanabe, H. Yoshida and M. Arai, *Appl. Catal., A*, 2014, **488**, 171–175.
- 188 M. M. Khin, A. S. Nair, V. J. Babu, R. Murugan and S. Ramakrishna, *Energy Environ. Sci.*, 2012, **5**, 8075–8109.
- 189 X. Hu, Y. Wu and Z. Zhang, *J. Mater. Chem.*, 2012, **22**, 15198–15205.
- 190 C. L. Mangun, J. A. DeBarr and J. Economy, *Carbon*, 2001, **39**, 1689–1696.
- 191 S. Kisamori, K. Kuroda, S. Kawano, I. Mochida, Y. Matsumura and M. Yoshikawa, *Energy Fuels*, 1994, **8**, 1337–1340.
- 192 S. J. Blanksby and G. B. Ellison, *Acc. Chem. Res.*, 2003, **36**, 255–263.
- 193 J. A. Labinger and J. E. Bercaw, *Nature*, 2002, **417**, 507–514.
- 194 X. Hu, Z. Zhou, Q. Lin, Y. Wu and Z. Zhang, *Chem. Phys. Lett.*, 2011, **503**, 287–291.